

Invertible Particle Flow-based Sequential MCMC With Extension To Gaussian Mixture Noise Models

Yunpeng Li, Soumyasundar Pal, and Mark Coates

Abstract—Sequential state estimation in non-linear and non-Gaussian state spaces has a wide range of applications in statistics and signal processing. One of the most effective non-linear filtering approaches, particle filtering, suffers from weight degeneracy in high-dimensional filtering scenarios. Several avenues have been pursued to address high-dimensionality. Among these, particle flow particle filters construct effective proposal distributions by using invertible flow to migrate particles continuously from the prior distribution to the posterior, and sequential Markov chain Monte Carlo (SMCMC) methods use a Metropolis-Hastings (MH) accept-reject approach to improve filtering performance. In this paper, we propose to combine the strengths of invertible particle flow and SMCMC by constructing a composite Metropolis-Hastings (MH) kernel within the SMCMC framework using invertible particle flow. In addition, we propose a Gaussian mixture model (GMM)-based particle flow algorithm to construct effective MH kernels for multi-modal distributions. Simulation results show that for high-dimensional state estimation example problems the proposed kernels significantly increase the acceptance rate with minimal additional computational overhead and improve estimation accuracy compared with state-of-the-art filtering algorithms.

I. INTRODUCTION

Effective and efficient on-line learning of high-dimensional states is an important task in many domains where we need to regularly update our knowledge by processing a deluge of streaming data. Relevant applications span from robotic learning to financial modelling, from multi-target tracking to weather forecasting [1]–[4]. In the presence of non-linear states space models, particle filters [5], [6] are one of the standard tools for sequential inference. However, it is in general difficult to construct effective proposal distributions to match well with the posterior distribution in high-dimensional spaces. A mismatch between the proposal and the posterior leads to negligible importance weights for most particles. These are normally discarded after resampling. This weight degeneracy issue thus leads to poor particle representation of the posterior and has limited the widespread application of particle filters in high-dimensional filtering scenarios [7]–[9].

Advanced particle filtering methods have been proposed to approximate the optimal proposal distribution [10] in order to alleviate the weight degeneracy issue. The *multiple particle filter* [11] partitions the state space into multiple

lower-dimensional spaces where state estimation is performed. The *block particle filter* takes a similar approach by partitioning the state space and the measurement space into independent blocks in updating the filtering distribution, although this introduces a bias that is difficult to quantify [12]. In [13], Beskos et al. introduced an unbiased *space-time particle filter* which also relies on factorization of the conditional posterior. These algorithms are promising but are applicable only in scenarios where the factorization can be performed. The *equivalent weights particle filter* sacrifices the statistical consistency to ensure substantial weights for a large number of particles [14]. *Particle flow filters* have been proposed to address high-dimensional filtering by transporting particles continuously from the prior to the posterior [15]–[18]. Most particle flow filters do not provide statistically consistent estimates of the posterior. Deterministic particle flow filters such as those we build on in this paper often underestimate the variance. Other versions incorporate approximation errors in the implementation or impose overly strong model assumptions [19], [20]. Recent stochastic particle flow filters such as those described in [18] address these limitations. As an alternative approach, [21]–[24] propose the use of particle flow or transport maps to construct a proposal distribution that approximates the posterior and then use importance sampling to correct for any discrepancy.

Another direction to combat weight degeneracy in high-dimensional filtering is to use Markov chain Monte Carlo (MCMC) methods to improve the diversity of samples. MCMC is often considered as the most effective method for sampling from a high-dimensional distribution [25]. More effective MCMC techniques in high-dimensional spaces use Hamiltonian or Langevin dynamics to construct efficient proposals [26]–[29]. Although effective, these techniques cannot be directly used in sequential inference tasks, as MCMC typically targets a static distribution. To use MCMC to diversify samples in a sequential setting, the resample-move particle filter incorporates MCMC methods by performing MCMC moves after the resampling step of the particle filter [30]. Unfortunately, the resampling step can lead to degeneracy, so many MCMC moves may be required to diversify particles.

A more general framework called sequential Markov chain Monte Carlo (SMCMC) uses MCMC techniques to sample directly from the approximate target distribution [31]–[34]. [31] directly targets the filtering distribution which is computationally expensive. [32]–[34] instead propose to sample from the joint state distribution to avoid the numerical integration of the predictive density. In the algorithms presented in [32]–[34], a fixed number of samples is used to approximate

Y. Li is with the Department of Computer Science, University of Surrey, Guildford, U.K., email: yunpeng.li@surrey.ac.uk; S. Pal and M. Coates are with the Department of Electrical and Computer Engineering, McGill University, Montréal, Québec, Canada, e-mail: soumyasundar.pal@mail.mcgill.ca; mark.coates@mcgill.ca. Y. Li and S. Pal are considered equal contributors. We acknowledge the support of the Natural Sciences and Engineering Research Council of Canada (NSERC) [2017-260250].

the empirical posterior distribution for each time step. By contrast, in the sequentially interacting MCMC (SIMCMC) framework described in [35], one can continue to generate interacting non-Markovian samples of the entire state sequence to improve the empirical approximation of joint posterior distribution successively. The resulting samples are asymptotically distributed according to the joint posterior distribution. The fundamental difference between the SMCMC and the SIMCMC techniques is that the SMCMC algorithm consists of sequential implementation of static MCMC schemes (justifying the name “sequential MCMC”), whereas this interpretation does not hold for the SIMCMC algorithm. Hence the analysis of SIMCMC in [35] cannot be applied to SMCMC (and vice-versa) and SMCMC cannot be expressed as a special case of SIMCMC. From a practical viewpoint, if a fixed number of particles is to be used, the effect of error in approximating the posterior distribution at the previous time step might be severe for the SIMCMC algorithm and limit its applicability in high dimensional online filtering problems compared to advanced SMC or SMCMC techniques.

A variety of MCMC kernels developed for sampling in high-dimensional spaces can be used inside the SMCMC framework. [34] and this paper differ from the past literature by using particle flow to construct MCMC kernels in the SMCMC framework.

In this paper, we propose to incorporate invertible particle flow [24] into the SMCMC framework. Our main contributions are three-fold: 1) we exploit the capability of particle flow to migrate samples into high posterior density regions to construct a composite Metropolis-Hasting (MH) kernel that significantly increases the acceptance rate of the joint draw; 2) for multi-modal distributions, we incorporate a Gaussian mixture model-based particle flow to improve sampling efficiency; 3) we assess the performance of the proposed methods through numerical simulation of challenging high-dimensional filtering examples. We presented preliminary results concerning an initial attempt to incorporate SMCMC with invertible particle flow in [34]. This paper provides a more detailed description of the proposed approach, presents more computationally efficient algorithms, and proposes a sequential MCMC method with mixture model-based flow for efficient exploration of multi-modal distributions. We also provide theoretical results regarding asymptotic convergence of the algorithms. These results are not restricted to the invertible particle flow composite kernel case, but hold for SMCMC methods provided the kernel and filtering problem satisfy certain assumptions (see Section IV-C). While similar in spirit to results presented in [35] for the SIMCMC algorithm, the key assumptions are slightly less restrictive and the theorem directly addresses the sequential implementation in [33] and this work. Recently, [36] carries out a rigorous statistical analysis of SMCMC algorithms to establish upper bounds on finite sample filter errors, in addition to providing asymptotic convergence results.

The rest of the paper is organized as follows. Section II provides the problem statement and Section III reviews the sequential MCMC framework and the invertible particle flow. We present the proposed methods in Section IV. Simulation examples and results are presented in Section V. We conclude

the paper in Section VI.

II. PROBLEM STATEMENT

Many online data analysis applications involve estimating unknown quantities, which we call the “state” x , given sequential measurements. Often there is prior knowledge related to the state x_0 , where the subscript 0 indicates the time step before any measurement arrives. A dynamic model describes the evolution of state $x_k \in \mathbb{R}^d$ at time step k given the past states and a measurement model captures the relationship between observations $z_k \in \mathbb{R}^S$ and the state x_k .

The hidden Markov model (HMM) is a ubiquitous tool for modelling the discrete-time dynamic system and measurement process. It is assumed that the hidden state x_k follows the Markov property, i.e., it is independent of all states before $k-1$ given the state x_{k-1} . The measurement z_k is modelled as independent of all past measurements and past states conditioned on the current state x_k . We can model the state evolution and measurements with the following HMM:

$$x_0 \sim p(x_0) , \quad (1)$$

$$x_k = g_k(x_{k-1}, v_k) \quad \text{for } k \geq 1 , \quad (2)$$

$$z_k = h_k(x_k, w_k) \quad \text{for } k \geq 1 . \quad (3)$$

Here $p(x_0)$ is the initial probability density function of the state x_0 , $g_k : \mathbb{R}^d \times \mathbb{R}^{d'} \rightarrow \mathbb{R}^d$ models the dynamics of the unobserved state x_k , and the measurement model $h_k : \mathbb{R}^d \times \mathbb{R}^{S'} \rightarrow \mathbb{R}^S$ describes the relation between the measurement z_k and the state x_k . We assume that $h_k(x_k, 0)$ is a C^1 function, i.e., $h_k(x_k, 0)$ is a differentiable function whose first derivative is continuous. $v_k \in \mathbb{R}^{d'}$ and $w_k \in \mathbb{R}^{S'}$ are the process noise and the measurement noise, respectively. With these models, the filtering task is to compute the posterior distribution of the state trajectory $p(x_k|z_1, \dots, z_k)$ online, as new data become available. For conciseness, we use $x_{a:b}$ to denote the set $\{x_a, x_{a+1}, \dots, x_b\}$ and $z_{a:b}$ to denote the set $\{z_a, z_{a+1}, \dots, z_b\}$, where a and b are integers and $a < b$. The posterior distribution $p(x_k|z_{1:k})$ gives a probabilistic interpretation of the state given all measurements, and can be used for state estimation and detection.

III. BACKGROUND MATERIAL

A. Sequential Markov chain Monte Carlo methods

Sequential Markov chain Monte Carlo (SMCMC) methods were proposed as a general MCMC approach for approximating the joint posterior distribution $\pi_k(x_{0:k}) = p(x_{0:k}|z_{1:k})$ recursively. A unifying framework of the various SMCMC methods was provided in [33]. At time step k , $\pi_k(x_{0:k})$ can be computed pointwise up to a constant in a recursive manner:

$$\begin{aligned} \pi_k(x_{0:k}) &= p(x_{0:k}|z_{1:k}) \propto p(x_{0:k}, z_{1:k}) , \\ &\propto p(x_k|x_{k-1})p(z_k|x_k)p(x_{0:k-1}|z_{1:k-1})p(z_{1:k-1}) , \\ &\propto p(x_k|x_{k-1})p(z_k|x_k)\pi_{k-1}(x_{0:k-1}) . \end{aligned} \quad (4)$$

As $\pi_{k-1}(x_{0:k-1})$ is not analytically tractable, it is impossible to sample from it in a general HMM. In all SMCMC methods, the distribution is replaced by its empirical approximation in (4), which leads to an approximation of π_k as follows:

$$\check{\pi}_k(x_{0:k}) \propto p(x_k|x_{k-1})p(z_k|x_k)\hat{\pi}_{k-1}(x_{0:k-1}) , \quad (5)$$

where

$$\widehat{\pi}_{k-1}(x_{0:k-1}) = \frac{1}{N_p} \sum_{j=N_b+1}^{N_b+N_p} \delta_{x_{k-1,0:k-1}^j}(x_{0:k-1}). \quad (6)$$

Here $\delta_a(\cdot)$ is the Dirac delta function centred at a , N_b is the number of samples discarded during a burn-in period, and N_p is the number of retained MCMC samples. $\{x_{k-1,0:k-1}^j\}_{j=N_b+1}^{N_b+N_p}$ are the N_p samples obtained from the Markov chain at time $k-1$, whose stationary distribution is $\check{\pi}_{k-1}(x_{0:k-1})$. At time step k , $N_b + N_p$ iterations of the Metropolis-Hastings (MH) algorithm with proposal $q_k(\cdot)$ are executed to generate samples $\{x_{k,0:k}^j\}_{j=N_b+1}^{N_b+N_p}$ from the invariant distribution $\check{\pi}_k(x_{0:k})$, and $\pi_k(x_{0:k})$ is approximated as:

$$\widehat{\pi}_k(x_{0:k}) = \frac{1}{N_p} \sum_{j=N_b+1}^{N_b+N_p} \delta_{x_{k,0:k}^j}(x_{0:k}) \quad (7)$$

The purpose of the joint draw of $\check{\pi}_k(x_{0:k})$ is to avoid numerical integration of the predictive density when the target distribution is $p(x_k|z_{1:k})$ [32]. Note that if we are only interested in approximating the marginal posterior distribution $p(x_k|z_{1:k})$, only $\{x_{k-1,k-1}^j\}_{j=N_b+1}^{N_b+N_p}$ needs to be stored instead of the full past state trajectories $\{x_{k-1,0:k-1}^j\}_{j=N_b+1}^{N_b+N_p}$. The Metropolis-Hastings (MH) algorithm used within SMCMC to generate one sample is summarized in Algorithm 1.

Algorithm 1: MH Kernel in SMCMC [33].

Input: $x_{k,0:k}^{i-1}$.

Output: $x_{k,0:k}^i$.

- 1: Propose $x_{k,0:k}^{*(i)} \sim q_k(x_{0:k}|x_{k,0:k}^{i-1})$;
 - 2: Compute the MH acceptance probability $\rho = \min\left(1, \frac{\check{\pi}_k(x_{k,0:k}^{*(i)})}{q_k(x_{k,0:k}^{*(i)}|x_{k,0:k}^{i-1})} \frac{q_k(x_{k,0:k}^{i-1}|x_{k,0:k}^{*(i)})}{\check{\pi}_k(x_{k,0:k}^{i-1})}\right)$;
 - 3: Accept $x_{k,0:k}^i = x_{k,0:k}^{*(i)}$ with probability ρ , otherwise set $x_{k,0:k}^i = x_{k,0:k}^{i-1}$;
-

1) *Composite MH kernel in SMCMC:* Different choices of the MCMC kernel for high dimensional SMCMC are discussed in [33]. In most SMCMC algorithms, an independent MH kernel is adopted [33], i.e., $q_k(x_{0:k-1}|x_{k,0:k}^{i-1}) = q_k(x_{0:k})$, meaning that the proposal is independent of the state of the Markov chain at the previous iteration. The ideal choice is the optimal independent MH kernel, but it is usually impossible to sample from [33]. It is difficult to identify an effective approximation to the optimal independent MH kernel. The choice of independent MH kernel using the prior as the proposal can lead to very low acceptance rates if the state dimension is very high or the measurements are highly informative.

[32], [33] propose the use of a composite MH kernel which is constituted of a joint proposal $q_{k,1}$ (to update $x_{0:k}$) followed by two individual state variable refinements using proposals $q_{k,2}$ (to update $x_{0:k-1}$) and $q_{k,3}$ (to update x_k), based on the *Metropolis within Gibbs* approach, within a single MCMC iteration. The composite kernel is summarized in Algorithm 2.

Algorithm 2: Composite MH Kernels in a unifying framework of SMCMC [32], [33].

Input: $x_{k,0:k}^{(i-1)}$

Output: $x_{k,0:k}^{(i)}$

Joint draw of $x_{k,0:k}^i$:

- 1: Propose $x_{k,0:k}^{*(i)} \sim q_{k,1}(x_{0:k}|x_{k,0:k}^{i-1})$;
 - 2: Compute the MH acceptance probability $\rho_1 = \min\left(1, \frac{\check{\pi}_k(x_{k,0:k}^{*(i)})}{q_{k,1}(x_{k,0:k}^{*(i)}|x_{k,0:k}^{i-1})} \frac{q_{k,1}(x_{k,0:k}^{i-1}|x_{k,0:k}^{*(i)})}{\check{\pi}_k(x_{k,0:k}^{i-1})}\right)$;
 - 3: Accept $x_{k,0:k}^i = x_{k,0:k}^{*(i)}$ with probability ρ_1 , otherwise set $x_{k,0:k}^i = x_{k,0:k}^{i-1}$;
- Individual refinement of $x_{k,0:k-1}^i$:
- 4: Propose $x_{k,0:k-1}^{*(i)} \sim q_{k,2}(x_{0:k-1}|x_{k,0:k}^i)$;
 - 5: Compute the MH acceptance probability $\rho_2 = \min\left(1, \frac{\check{\pi}_k(x_{k,0:k-1}^{*(i)}, x_{k,k}^i)}{q_{k,2}(x_{k,0:k-1}^{*(i)}|x_{k,0:k}^i)} \frac{q_{k,2}(x_{k,0:k-1}^i|x_{k,0:k-1}^{*(i)}, x_{k,k}^i)}{\check{\pi}_k(x_{k,0:k}^i)}\right)$;
 - 6: Accept $x_{k,0:k-1}^i = x_{k,0:k-1}^{*(i)}$ with probability ρ_2 ;
- Individual refinement of $x_{k,k}^i$:
- 7: Propose $x_{k,k}^{*(i)} \sim q_{k,3}(x_k|x_{k,0:k}^i)$;
 - 8: Compute the MH acceptance probability $\rho_3 = \min\left(1, \frac{\check{\pi}_k(x_{k,0:k-1}^i, x_{k,k}^{*(i)})}{q_{k,3}(x_{k,k}^{*(i)}|x_{k,0:k}^i)} \frac{q_{k,3}(x_{k,k}^i|x_{k,0:k-1}^i, x_{k,k}^{*(i)})}{\check{\pi}_k(x_{k,0:k}^i)}\right)$;
 - 9: Accept $x_{k,k}^i = x_{k,k}^{*(i)}$ with probability ρ_3 ;
-

Any of the MCMC kernels mentioned before can be used in the joint draw step of a composite kernel. For example, the independent MH kernel based on the prior as the proposal is used in the joint draw step of the implementation of the sequential manifold Hamiltonian Monte Carlo (SmHMC) algorithm in [33]. For individual refinement of $x_{k,0:k-1}^i$, [33] uses the independent proposal $q_{k,2} = \widehat{\pi}_{k-1}$, which leads to the following simplification of MH acceptance rate in Line 5 of Algorithm 1, using Equation (5).

$$\begin{aligned} \rho_2 &= \min\left(1, \frac{\check{\pi}_k(x_{k,0:k-1}^{*(i)}, x_{k,k}^i) \widehat{\pi}_{k-1}(x_{k,0:k-1}^i)}{\widehat{\pi}_{k-1}(x_{k,0:k-1}^{*(i)}) \check{\pi}_k(x_{k,0:k}^i)}\right) \\ &= \min\left(1, \frac{p(x_{k,k}^i|x_{k,k-1}^{*(i)})}{p(x_{k,k}^i|x_{k,k-1}^i)}\right). \end{aligned} \quad (8)$$

The aim of the refinement steps is to explore the neighbourhood of samples generated in the joint draw step. For the MCMC kernel of the individual refinement step of x_k , Langevin diffusion or Hamiltonian dynamics have been proposed to more efficiently traverse a high-dimensional space [33]. The manifold Hamiltonian Monte Carlo (mHMC) kernel $q_{k,3}(\cdot)$ of the individual refinement step of the SmHMC algorithm efficiently samples from the target filtering distribution, making the SmHMC algorithm one of the most effective algorithms for filtering in high-dimensional spaces.

B. Particle flow particle filter

1) *Particle flow filter:* In the last decade, a new class of Monte Carlo-based filters has emerged that shows promise in

high-dimensional filtering. In a given time step k , particle flow algorithms [15], [19] migrate particles from the predictive distribution $p(x_k|z_{1:k-1})$ to the posterior distribution $p(x_k|z_{1:k})$, via a ‘‘flow’’ that is specified through a partial differential equation (PDE). There is no sampling (or resampling). Thus the weight degeneracy issue is avoided.

A particle flow can be modelled by a background stochastic process η_λ in a pseudo-time interval $\lambda \in [0, 1]$, such that the distribution of η_0 is the predictive distribution $p(x_k|z_{1:k-1})$ and the distribution of η_1 is the posterior distribution $p(x_k|z_{1:k}) = \frac{p(x_k|z_{1:k-1})p(z_k|x_k)}{p(z_k|z_{1:k-1})}$.

In [19], the underlying equation stochastic process η_λ satisfies an ordinary differential equation (ODE) with zero diffusion:

$$\frac{d\eta_\lambda}{d\lambda} = \varphi(\eta_\lambda, \lambda). \quad (9)$$

When the predictive distribution and the likelihood are both Gaussian, the exact flow for the linear Gaussian model is:

$$\varphi(\eta_\lambda, \lambda) = \frac{d\eta_\lambda}{d\lambda} = A(\lambda)\eta_\lambda + b(\lambda), \quad (10)$$

where

$$A(\lambda) = -\frac{1}{2}PH^T(\lambda HPH^T + R)^{-1}H, \quad (11)$$

$$b(\lambda) = (I + 2\lambda A(\lambda))[(I + \lambda A(\lambda))PH^TR^{-1}z + A(\lambda)\bar{\eta}_0], \quad (12)$$

Here $\bar{\eta}_0$ is the mean of the predictive distribution, P is the covariance matrix of prediction error for the prior distribution, z is the new measurement, H is the measurement matrix, i.e. $h_k(x_k) = Hx_k$, and R is the covariance matrix of the measurement noise. We refer to this method as the exact Daum-Huang (EDH) filter, and a detailed description of its implementation is provided in [37]. For nonlinear models, a computationally intensive variation of EDH, that computes a separate flow for each particle by performing linearization at the particle location η_λ^i , was proposed in [16] and is referred to as the localized exact Daum-Huang (LEDH) filter.

Numerical integration is normally used to solve the ODE in Equation (9). The integral between λ_{j-1} and λ_j for $1 \leq j \leq N_\lambda$, where $\lambda_0 = 0$ and $\lambda_{N_\lambda} = 1$, is approximated and the Euler update rule for the EDH flow becomes

$$\begin{aligned} \eta_{\lambda_j}^i &= f_{\lambda_j}(\eta_{\lambda_{j-1}}^i) \\ &= \eta_{\lambda_{j-1}}^i + \epsilon_j(A(\lambda_j)\eta_{\lambda_{j-1}}^i + b(\lambda_j)), \end{aligned} \quad (13)$$

where the step size $\epsilon_j = \lambda_j - \lambda_{j-1}$ and $\sum_{j=1}^{N_\lambda} \epsilon_j = 1$.

2) *Particle flow particle filter*: Because of the discretization errors made while numerically solving Eq (9), and the mismatch of modelling assumptions between a general HMM and a linear Gaussian setup (which was assumed in deriving Equations (11) and (12)), the migrated particles after the particle flow process are not exactly distributed according to the posterior. Instead η_1^i can be viewed as being drawn from a proposal distribution $q(\eta_1^i|x_{k-1}^i, z_k)$, which is possibly well matched to the posterior, because of the flow procedure. It is shown in [24] that for the EDH, if an auxiliary flow is

performed starting from the mean of the predictive distribution $\bar{\eta}_0$, and the generated flow parameters are used to perform particle flow for each particle η_0^i , then in presence of the assumed smoothness condition on the measurement function h and with sufficiently small step sizes ϵ_j , the auxiliary particle flow establishes an invertible mapping $\eta_1^i = T(\eta_0^i; z_k, x_{k-1}^i)$. We can straightforwardly compute the proposal density as follows:

$$q(\eta_1^i|x_{k-1}^i, z_k) = \frac{p(\eta_0^i|x_{k-1}^i)}{|\det(\dot{T}(\eta_0^i; x_{k-1}^i, z_k))|}, \quad (14)$$

$\dot{T}(\cdot) \in \mathbb{R}^{d \times d}$ is the Jacobian determinant of the mapping function $T(\cdot)$ and $|\cdot|$ denotes the absolute value. The determinant of $\dot{T}(\cdot)$ is given as:

$$\det(\dot{T}(\eta_0^i; x_{k-1}^i, z_k)) = \prod_{j=1}^{N_\lambda} \det(I + \epsilon_j A(\lambda_j)) \quad (15)$$

3) *Particle flow particle filter with Gaussian mixture model assumptions*: When the state space models involve Gaussian mixture model (GMM) noise, Equations (2) and (3) admit the following structures $v_k \sim \sum_{m=1}^M \alpha_{k,m} \mathcal{N}(\psi_{k,m}, Q_{k,m})$ and $w_k \sim \sum_{n=1}^N \beta_{k,n} \mathcal{N}(\zeta_{k,n}, R_{k,n})$.

An alternative representation of the GMM allows an equivalent formulation of the dynamic model by introducing a latent scalar variable $d_k \in \{1, 2, \dots, M\}$ with a probability mass function (PMF) $p(d_k = m) = \alpha_{k,m}$. The variable d_k specifies the GMM component that excites the dynamic model, i.e., $p(x_k|x_{k-1}, d_k = m) = \mathcal{N}(x_k|g_k(x_{k-1}) + \psi_{k,m}, Q_{k,m})$. The state transition density can then be described as:

$$\begin{aligned} p(x_k|x_{k-1}) &= \sum_{m=1}^M p(d_k = m)p(x_k|x_{k-1}, d_k = m) \\ &= \sum_{m=1}^M \alpha_{k,m} \mathcal{N}(x_k|g_k(x_{k-1}) + \psi_{k,m}, Q_{k,m}). \end{aligned} \quad (16)$$

Similarly, a latent variable c_k with the PMF $p(c_k = n) = \beta_{k,n}$ specifies the GMM component that generates the measurement noise. The likelihood can be described as follows:

$$\begin{aligned} p(z_k|x_k) &= \sum_{n=1}^N p(c_k = n)p(z_k|x_k, c_k = n) \\ &= \sum_{n=1}^N \beta_{k,n} \mathcal{N}(z_k|h_k(x_k) + \zeta_{k,n}, R_{k,n}). \end{aligned} \quad (17)$$

In order to construct the particle flow particle filter for this model, at time step k , first $d_k^i = m \in \{1, 2, \dots, M\}$ is sampled with probability $\{\alpha_{k,1}, \alpha_{k,2}, \dots, \alpha_{k,M}\}$ and $c_k^i = n \in \{1, 2, \dots, N\}$ is sampled with probability $\{\beta_{k,1}, \beta_{k,2}, \dots, \beta_{k,N}\}$. Conditioned on (d_k^i, c_k^i) , an invertible particle flow $(A_{mn}^i(\lambda), b_{mn}^i(\lambda))$ based on LEDH is constructed using the m -th and n -th Gaussian components of the dynamic and measurement models respectively, to sample x_k^i . The importance weights of the joint state $\{x_k, d_k, c_k\}$ can be updated as follows [38]:

$$\omega_k^i \propto \omega_{k-1}^i \frac{p(x_k^i|x_{k-1}^i, d_k^i)p(z_k|x_k^i, c_k^i)}{q(x_k^i|x_{k-1}^i, d_k^i, c_k^i, z_k)} \quad (18)$$

where the proposal density is computed by:

$$q(x_k^i|x_{k-1}^i, d_k^i = m, c_k^i = n, z_k) = \frac{p(\eta_0^i|x_{k-1}^i, d_k^i = m)}{|\prod_{j=1}^{N_\lambda} \det(I + \epsilon_j A_{mn}^i(\lambda_j))|}. \quad (19)$$

IV. METHODS

In this section, we propose to use the invertible particle flow to approximate the optimal independent MH kernel in the sequential MCMC methods for both uni-modal and multi-modal target distributions.

A. SMCMC with invertible particle flow

To construct MH kernels based on invertible particle flow, we first develop a new formulation of the invertible mapping with particle flow.

1) *New formulation of the invertible mapping with particle flow*: The particle flow particle filters (PF-PFs) construct invertible particle flows in a pseudo-time interval $\lambda \in [0, 1]$ in order to move particles drawn from the prior distribution into regions where the posterior density is high.

Using the Euler update rule specified in Equation (13) recursively over $j = N_\lambda, N_\lambda - 1, \dots, 2, 1$, the invertible mapping for the PF-PF (EDH) can be expressed as:

$$\begin{aligned} \eta_1^i &= f_{\lambda_{N_\lambda}}(f_{\lambda_{N_\lambda-1}}(\dots f_{\lambda_1}(\eta_0^i))) \\ &= (I + \epsilon_{N_\lambda} A(\lambda_{N_\lambda})) \eta_{\lambda_{N_\lambda-1}}^i + \epsilon_{N_\lambda} b(\lambda_{N_\lambda}) \\ &= \dots \\ &= C \eta_0^i + D, \end{aligned} \quad (20)$$

where

$$C = \prod_{j=1}^{N_\lambda} (I + \epsilon_{N_\lambda+1-j} A(\lambda_{N_\lambda+1-j})), \quad (21)$$

and

$$D = \epsilon_{N_\lambda} b(\lambda_{N_\lambda}) + \sum_{m=1}^{N_\lambda-1} \left(\prod_{j=1}^{N_\lambda-m} (I + \epsilon_{N_\lambda+1-j} A(\lambda_{N_\lambda+1-j})) \right) \epsilon_j b(\lambda_j). \quad (22)$$

In [24] it is shown that the equivalent mapping is invertible with sufficiently small ϵ_j , so the matrix C is invertible. The procedure to produce C and D is summarized in Algorithm 3 and the proposal density becomes

$$q(\eta_1^i | x_{k-1}^i, z_k) = \frac{p(\eta_0^i | x_{k-1}^i)}{|\det(C)|}. \quad (23)$$

Algorithm 3: Function(C, D) = $F(\bar{\eta})$

- 1: Initialize: $C = I, D = \mathbf{0}$;
 - 2: **for** $j = 1, \dots, N_\lambda$ **do**
 - 3: Set $\lambda_j = \lambda_{j-1} + \epsilon_j$;
 - 4: Calculate $A(\lambda_j)$ and $b(\lambda_j)$ with the linearization being performed at $\bar{\eta}$;
 - 5: Migrate $\bar{\eta}$: $\bar{\eta} = \bar{\eta} + \epsilon_j (A(\lambda_j) \bar{\eta} + b(\lambda_j))$;
 - 6: Set $C = (I + \epsilon_j A(\lambda_j)) C$;
 - 7: Set $D = (I + \epsilon_j A(\lambda_j)) D + \epsilon_j b(\lambda_j)$;
 - 8: **end for**
-

Similarly, for the PF-PF (LEDH), the invertible mapping can be expressed as

$$\eta_1^i = C^i \eta_0^i + D^i, \quad (24)$$

where $(C^i, D^i) = F(\bar{\eta}_0^i)$. In this expression, $\bar{\eta}_0^i = g_k(x_{k-1}^i, 0)$ where $g_k(\cdot, \cdot)$ is the dynamic model introduced in Equation (2). The proposal density becomes

$$q(\eta_1^i | x_{k-1}^i, z_k) = \frac{p(\eta_0^i | x_{k-1}^i)}{|\det(C^i)|}. \quad (25)$$

2) *SmHMC with LEDH*: One of the composite MH kernels we propose uses the invertible particle flow based on the LEDH flow and is presented in Algorithm 4.

Algorithm 4: Composite MH Kernels constructed with the manifold Hamiltonian Monte Carlo kernel and the invertible particle flow with LEDH, at the i -th MCMC iteration of k -th time step.

Input: $x_{k,0:k}^{i-1}, \eta_0^{i-1}, C^{i-1}$.

Output: $x_{k,0:k}^i, \eta_0^i, C^i$.

Joint draw of $x_{k,0:k}^i$:

- 1: Draw $x_{k,0:k-1}^{*(i)} \sim \hat{\pi}_{k-1}(x_{0:k-1})$;
 - 2: Sample $\eta_0^{*(i)} = g_k(x_{k,k-1}^{*(i)}, v_k)$, calculate $\bar{\eta}_0^{*(i)} = g_k(x_{k,k-1}^{*(i)}, 0)$;
 - 3: Perform invertible particle flow (Algorithm 3) $(C^{*(i)}, D^{*(i)}) = F(\bar{\eta}_0^{*(i)})$;
 - 4: Calculate $x_{k,k}^{*(i)} = C^{*(i)} \eta_0^{*(i)} + D^{*(i)}$;
 - 5: Compute the MH acceptance probability $\rho_1 = \min\left(1, \frac{p(x_{k,k}^{*(i)} | x_{k,k-1}^{*(i)}) p(z_k | x_{k,k}^{*(i)}) |\det(C^{*(i)})| p(\eta_0^{i-1} | x_{k,k-1}^{i-1})}{p(\eta_0^{*(i)} | x_{k,k-1}^{*(i)}) p(x_{k,k-1}^{i-1} | x_{k,k-1}^{*(i)}) p(z_k | x_{k,k}^{i-1}) |\det(C^{i-1})|}\right)$;
 - 6: Accept $x_{k,0:k}^i = x_{k,0:k}^{*(i)}, \eta_0^i = \eta_0^{*(i)}, C^i = C^{*(i)}$ and $D^i = D^{*(i)}$ with probability ρ_1 .
Otherwise set $x_{k,0:k}^i = x_{k,0:k}^{i-1}, \eta_0^i = \eta_0^{i-1}, C^i = C^{i-1}$ and $D^i = D^{i-1}$;
 - 7: Individual refinements of $x_{k,0:k}^i$ using Algorithm 5;
 - 8: Calculate $\eta_0^i = (C^i)^{-1}(x_{k,k}^i - D^i)$;
-

Algorithm 5: Individual refinement steps of composite MH Kernels constructed with the manifold Hamiltonian Monte Carlo kernel, at the i -th MCMC iteration of k -th time step.

Input: $x_{k,0:k}^i$.

Output: $x_{k,0:k}^i$.

Individual refinement of $x_{k,0:k-1}^i$:

- 1: Draw $x_{k,0:k-1}^{*(i)} \sim \hat{\pi}_{k-1}(x_{0:k-1})$;
 - 2: Compute the MH acceptance probability $\rho_2 = \min\left(1, \frac{p(x_{k,k}^i | x_{k,k-1}^{*(i)})}{p(x_{k,k}^{*(i)} | x_{k,k-1}^{*(i)})}\right)$;
 - 3: Accept $x_{k,0:k-1}^i = x_{k,0:k-1}^{*(i)}$ with probability ρ_2 ;
- Individual refinement of $x_{k,k}^i$:
- 4: Propose $x_{k,k}^{*(i)} \sim q_{k,3}(x_k | x_{k,k-1:k}^i, z_k)$ using the manifold Hamiltonian MCMC kernel;
 - 5: Compute the MH acceptance probability $\rho_3 = \min\left(1, \frac{p(x_{k,k}^{*(i)} | x_{k,k-1}^i) p(z_k | x_{k,k}^{*(i)}) q_{k,3}(x_{k,k}^i | x_{k,k-1}^i, x_{k,k}^{*(i)}, z_k)}{q_{k,3}(x_{k,k}^{*(i)} | x_{k,k-1:k}^i, z_k) p(x_{k,k}^i | x_{k,k-1}^i) p(z_k | x_{k,k}^i)}\right)$;
 - 6: Accept $x_{k,k}^i = x_{k,k}^{*(i)}$ with probability ρ_3 ;
-

In the i -th MCMC iteration at time step k , we first sample $x_{k,0:k-1}^{*(i)} \sim \widehat{\pi}_{k-1}(x_{0:k-1})$ from the approximate joint posterior distribution at time $k-1$. Then, we calculate $\eta_0^{*(i)} = g_k(x_{k,k-1}^{*(i)}, 0)$ to obtain the auxiliary LEDH flow parameters $(C^{*(i)}, D^{*(i)}) = F(\eta_0^{*(i)})$, and apply the flow to the propagated particle $\eta_0^{*(i)} = g_k(x_{k,k-1}^{*(i)}, v_k)$. Thus the proposed particle is generated as: $x_{k,k}^{*(i)} = \eta_1^{*(i)} = C^{*(i)}\eta_0^{*(i)} + D^{*(i)}$.

For this proposal, the acceptance rate of the joint draw in Algorithm 4 can be derived using Equations (5) and (25):

$$\begin{aligned} \rho_1 &= \min \left(1, \frac{\check{\pi}_k(x_{k,0:k}^{*(i)})\widehat{\pi}_{k-1}(x_{k,0:k-1}^{i-1})q(x_{k,k}^{i-1}|x_{k-1}^{i-1}, z_k)}{\widehat{\pi}_{k-1}(x_{k,0:k-1}^{*(i)})q(x_{k,k}^{*(i)}|x_{k-1}^{*(i)}, z_k)\check{\pi}_k(x_{k,0:k}^{i-1})} \right), \\ &= 1 \wedge \frac{p(x_{k,k}^{*(i)}|x_{k,k-1}^{*(i)})p(z_k|x_{k,k}^{*(i)})|\det(C^{*(i)})|p(\eta_0^{i-1}|x_{k,k-1}^{i-1})}{p(\eta_0^{*(i)}|x_{k,k-1}^{*(i)})p(x_{k,k}^{i-1}|x_{k,k-1}^{i-1})p(z_k|x_{k,k}^{i-1})|\det(C^{i-1})|}, \end{aligned} \quad (26)$$

where we use \wedge to denote the minimum operator.

When evaluating Equation (26) in Line 5 of Algorithm 4, the values of $x_{k,k}^{i-1}$, η_0^{i-1} and C^{i-1} are needed. Since $x_{k,k}^{i-1}$ may be generated by the manifold Hamiltonian Monte Carlo kernel $q_{k,3}(\cdot)$ as shown in Algorithm 5, the corresponding η_0^{i-1} is not available through Lines 2 and 6 of Algorithm 4. This can be resolved using the invertible mapping property of the invertible particle flow. As C^{i-1} is invertible, we can calculate η_0^{i-1} given $x_{k,k}^{i-1}$ by solving Equation (24):

$$\eta_0^{i-1} = (C^{i-1})^{-1}(x_{k,k}^{i-1} - D^{i-1}). \quad (27)$$

3) *SmHMC with EDH*: Calculation of individual flow parameters at every MCMC iteration in Algorithm 4 can be computationally expensive. Similar to the spirit of the PF-PF (EDH) [24], we can calculate the flow parameters C and D only once, using an auxiliary state variable derived from the samples, and apply the calculated flow parameters for all MCMC iterations. The resulting procedure is described in Algorithm 6. The flow parameters C and D are calculated only once in the initialization of each time step k , as in Algorithm 7.

The calculation of the acceptance rate in the joint draw step can be further simplified compared to Equation (26) as the same mapping of the flow is applied to each particle. The candidate particle $x_{k,k}^{*(i)}$ and the particle $x_{k,k}^{i-1}$ share the same value of C in their proposal densities (Equation (23)). Thus, for the SmHMC algorithm with the EDH flow, we have

$$\rho_1 = \min \left(1, \frac{p(x_{k,k}^{*(i)}|x_{k,k-1}^{*(i)})p(z_k|x_{k,k}^{*(i)})p(\eta_0^{i-1}|x_{k,k-1}^{i-1})}{p(\eta_0^{*(i)}|x_{k,k-1}^{*(i)})p(x_{k,k}^{i-1}|x_{k,k-1}^{i-1})p(z_k|x_{k,k}^{i-1})} \right). \quad (28)$$

B. SmHMC with LEDH for GMM distributed noises

When the process and measurement noises are distributed as Gaussian mixtures, the posterior distribution $\pi_k(x_{0:k})$ becomes multi-modal. In order to explore different modes of

Algorithm 6: Composite MH Kernels constructed with the manifold Hamiltonian Monte Carlo kernel and the invertible particle flow with EDH, at the i -th MCMC iteration of k -th time step. C and D were pre-computed using Algorithm 7.

Input: $x_{k,0:k}^{i-1}, \eta_0^{i-1}, C, D$.

Output: $x_{k,0:k}^i, \eta_0^i$.

Joint draw of $x_{k,0:k}^i$:

- 1: Draw $x_{k,0:k-1}^{*(i)} \sim \widehat{\pi}_{k-1}(x_{0:k-1})$;
 - 2: Sample $\eta_0^{*(i)} = g_k(x_{k,k-1}^{*(i)}, v_k)$;
 - 3: Calculate $x_{k,k}^{*(i)} = C\eta_0^{*(i)} + D$;
 - 4: Compute the MH acceptance probability $\rho_1 = \min \left(1, \frac{p(x_{k,k}^{*(i)}|x_{k,k-1}^{*(i)})p(z_k|x_{k,k}^{*(i)})p(\eta_0^{i-1}|x_{k,k-1}^{i-1})}{p(\eta_0^{*(i)}|x_{k,k-1}^{*(i)})p(x_{k,k}^{i-1}|x_{k,k-1}^{i-1})p(z_k|x_{k,k}^{i-1})} \right)$;
 - 5: Accept $x_{k,0:k}^i = x_{k,0:k}^{*(i)}$, $\eta_0^i = \eta_0^{*(i)}$ with probability ρ_1 .
Otherwise set $x_{k,0:k}^i = x_{k,0:k}^{i-1}$, $\eta_0^i = \eta_0^{i-1}$;
 - 6: Individual refinements of $x_{k,0:k}^i$ using Algorithm 5;
 - 7: Calculate $\eta_0^i = C^{-1}(x_{k,k}^i - D)$;
-

Algorithm 7: The flow parameter calculation for SmHMC (EDH).

- 1: Draw $x_{k,0:k-1}^0 \sim \widehat{\pi}_{k-1}(x_{0:k-1})$;
 - 2: Sample $\eta_0^0 = g_k(x_{k,k-1}^0, v_k)$,
calculate $\bar{\eta}_0 = g_k(\bar{x}_{k-1,k-1}, 0)$;
 - 3: Perform invertible particle flow (Algorithm 3)
(C, D) = $F(\bar{\eta}_0)$;
-

the posterior efficiently, we consider an extended state-space (x_k, d_k, c_k) , as in [38], and define the joint posterior as

$$\begin{aligned} \pi_k(x_{0:k}, d_{1:k}, c_{1:k}) &= p(x_{0:k}, d_{1:k}, c_{1:k}|z_{1:k}), \\ &\propto p(d_k)p(c_k)p(x_k|x_{k-1}, d_k)p(z_k|x_k, c_k) \times \\ &\quad \pi_{k-1}(x_{0:k-1}, d_{1:k-1}, c_{1:k-1}), \end{aligned} \quad (29)$$

which admits $\pi_k(x_{0:k})$ as its $x_{0:k}$ marginal. Similar to Equation (5), based on the approximate joint posterior $\widehat{\pi}_{k-1}(x_{0:k-1}, d_{1:k-1}, c_{1:k-1})$, of the previous time step $k-1$, we approximate $\pi_k(x_{0:k}, d_{1:k}, c_{1:k})$ as follows:

$$\begin{aligned} \check{\pi}(x_{0:k}, d_{1:k}, c_{1:k}) &\propto p(d_k)p(c_k)p(x_k|x_{k-1}, d_k)p(z_k|x_k, c_k) \\ &\quad \times \widehat{\pi}_{k-1}(x_{0:k-1}, d_{1:k-1}, c_{1:k-1}). \end{aligned} \quad (30)$$

For this model, in the joint draw step of SMCMC, we adopt the following strategy. First we sample

$$(x_{k,0:k-1}^{*(i)}, d_{k,1:k-1}^{*(i)}, c_{k,1:k-1}^{*(i)}) \sim \widehat{\pi}_{k-1}(x_{0:k-1}, d_{1:k-1}, c_{1:k-1}). \quad (31)$$

Similar to the spirit of auxiliary particle filtering [39], we design efficient measurement-driven proposals for sampling (d_k, c_k) , in contrast to [38], where the switching variables are sampled from their respective priors. To sample $d_{k,k}^{*(i)}$, we use the following proposal:

$$\begin{aligned} q(d_{k,k}^{*(i)} = m|x_{k,k-1}^{*(i)}, z_k) &\propto p(d_{k,k}^{*(i)} = m) \\ &\quad \times p(\bar{\eta}_0^{*(i)}|x_{k,k-1}^{*(i)}, d_{k,k}^{*(i)} = m)p(z_k|\bar{\eta}_0^{*(i)}), \end{aligned} \quad (32)$$

where $\bar{\eta}_0^{*(i)} = g_k(x_{k,k-1}^{*(i)}, \psi_{k,m})$. Conditioned on $d_{k,k}^{*(i)} = m$, we sample $c_{k,k}^{*(i)}$ from

$$q(c_{k,k}^{*(i)} = n | x_{k,k-1}^{*(i)}, d_{k,k}^{*(i)} = m, z_k) \propto p(c_{k,k}^{*(i)} = n) \times p(z_k | \bar{\eta}_0^{*(i)}, c_{k,k}^{*(i)} = n). \quad (33)$$

Then conditioned on $(d_{k,k}^{*(i)} = m, c_{k,k}^{*(i)} = n)$, we calculate $\bar{\eta}_0^{*(i)} = g_k(x_{k,k-1}^{*(i)}, \psi_{k,m})$ to obtain the auxiliary LEDH flow parameters $(C^{*(i)}, D^{*(i)}) = F(\bar{\eta}_0^{*(i)})$, using the m -th and n -th Gaussian component of the dynamic and measurement model respectively. Then this flow is applied to the propagated particle $\eta_0^{*(i)} = g_k(x_{k,k-1}^{*(i)}, v_{k,m})$, where $v_{k,m} \sim \mathcal{N}(\psi_{k,m}, Q_{k,m})$ is the m -th component in the process noise. The proposed particle is generated as: $x_{k,k}^i = \eta_1^{*(i)} = C^{*(i)}\eta_0^{*(i)} + D^{*(i)}$. Using the invertible mapping property, established by the flow, we can calculate

$$q(x_{k,k}^{*(i)} | x_{k,k-1}^{*(i)}, d_{k,k}^{*(i)} = m, c_{k,k}^{*(i)} = n, z_k) = \frac{p(\bar{\eta}_0^{*(i)} | x_{k,k-1}^{*(i)}, d_{k,k}^{*(i)} = m)}{|\det(C^{*(i)})|}. \quad (34)$$

Using Equations (30), (32), (33) and (34), the acceptance rate for the joint draw of $(x_{k,0:k}^{*(i)}, d_{k,1:k}^{*(i)}, c_{k,1:k}^{*(i)})$ using the proposed kernel can be calculated as:

$$\rho_1 = \min \left(1, \frac{p(d_{k,k}^{*(i)})p(c_{k,k}^{*(i)})p(x_{k,k}^{*(i)} | x_{k,k-1}^{*(i)}, d_{k,k}^{*(i)})}{q(d_{k,k}^{*(i)} | x_{k,k-1}^{*(i)}, z_k)q(c_{k,k}^{*(i)} | x_{k,k-1}^{*(i)}, d_{k,k}^{*(i)})} \times \frac{q(d_{k,k}^{i-1} | x_{k,k-1}^{i-1}, z_k)q(c_{k,k}^{i-1} | x_{k,k-1}^{i-1}, d_{k,k}^{i-1})}{p(d_{k,k}^{i-1})p(c_{k,k}^{i-1})p(x_{k,k}^{i-1} | x_{k,k-1}^{i-1}, d_{k,k}^{i-1})} \times \frac{|\det(C^{*(i)})|p(\bar{\eta}_0^{i-1} | x_{k,k-1}^{i-1}, d_{k,k}^{i-1})p(z_k | x_{k,k}^{*(i)}, c_{k,k}^{*(i)})}{p(\bar{\eta}_0^{*(i)} | x_{k,k-1}^{*(i)}, d_{k,k}^{*(i)})|\det(C^{i-1})|p(z_k | x_{k,k}^{i-1}, c_{k,k}^{i-1})} \right). \quad (35)$$

For individual refinement of $x_{k,0:k-1}^i$, we use the independent proposal $q_{k,2} = \hat{\pi}_{k-1}$. We can compute the acceptance rate of the refinement as follows:

$$\rho_2 = \min \left(1, \frac{\tilde{\pi}_k(x_{k,0:k-1}^i, x_{k,k}^i, d_{k,1:k}^i, c_{k,1:k}^i)}{\tilde{\pi}_{k-1}(x_{k,0:k-1}^i)} \frac{\tilde{\pi}_{k-1}(x_{k,0:k-1}^i)}{\tilde{\pi}_k(x_{k,0:k}^i, d_{k,1:k}^i, c_{k,1:k}^i)} \right) = \min \left(1, \frac{p(x_{k,k}^i | x_{k,k-1}^i, d_{k,k}^i)}{p(x_{k,k}^i | x_{k,k-1}^i, d_{k,k}^i)} \right). \quad (36)$$

The algorithm is summarized in Algorithm 8. From Equation (35), we note that we can discard $\{(d_{k,k}^j, c_{k,k}^j)\}_{j=N_b+1}^{N_b+N_p}$ after every time step k , if we are only interested in approximating $\pi_k(x_{0:k})$.

C. Convergence results

In this section, we present some theoretical results regarding convergence of the approximate joint posterior distribution $\hat{\pi}_k(x_{0:k})$ to $\pi_k(x_{0:k})$ for every $k \geq 0$. As in Section III, we use $\pi_k(x_{0:k})$ to denote our target distribution $p(x_{0:k} | z_{1:k})$. We initialize by setting $\pi_0(x_0) = p(x_0)$. To facilitate concise presentation of the results, we use a simplified notation in this subsection and Appendices A and B, where $x_{0:k}^i$ and $x_{0:k}^{*(i)}$ denote $x_{k,0:k}^i$ and $x_{k,0:k}^{*(i)}$, respectively. We also use $\hat{\pi}_k^{(N_p)}$ and $\tilde{\pi}_k^{(N_p)}$ to denote $\hat{\pi}_k$ and $\tilde{\pi}_k$ to indicate explicitly that they are comprised of N_p MCMC samples. While proving the theorems, we assume that the burn-in period $N_b = 0$, for

Algorithm 8: Composite MH Kernels for models with Gaussian mixture noises, constructed with the manifold Hamiltonian Monte Carlo kernel and the invertible particle flow with LEDH, at the i -th MCMC iteration of k -th time step.

Input: $x_{k,0:k}^{i-1}, \eta_0^{i-1}, d_{k,k}^{i-1}, c_{k,k}^{i-1}, C^{i-1}$.

Output: $x_{k,0:k}^i, \eta_0^i, d_{k,k}^i, c_{k,k}^i, C^i$.

Joint draw of $x_{k,0:k}^i$:

- 1: Draw $x_{k,0:k-1}^{*(i)} \sim \hat{\pi}_{k-1}(x_{0:k-1})$;
- 2: Sample $d_{k,k}^{*(i)} = m \in \{1, 2, \dots, M\}$ from $q(d_{k,k} | x_{k,k-1}^{*(i)}, z_k)$;
- 3: Sample $\eta_0^{*(i)} = g_k(x_{k,k-1}^{*(i)}, v_{k,m})$, where $v_{k,m} \sim \mathcal{N}(\psi_{k,m}, Q_{k,m})$, calculate $\bar{\eta}_0^{*(i)} = g_k(x_{k,k-1}^{*(i)}, \psi_{k,m})$;
- 4: Sample $c_{k,k}^{*(i)} = n \in \{1, 2, \dots, N\}$ from $q(c_{k,k} | x_{k,k-1}^{*(i)}, d_{k,k}^{*(i)} = m, z_k)$;
- 5: Perform invertible particle flow (Algorithm 3) $(C^{*(i)}, D^{*(i)}) = F(\bar{\eta}_0^{*(i)})$ using m -th and n -th component of dynamic and measurement models respectively;
- 6: Calculate $x_{k,k}^{*(i)} = C^{*(i)}\eta_0^{*(i)} + D^{*(i)}$;
- 7: Compute the MH acceptance probability $\rho_1 = \min \left(1, \frac{p(d_{k,k}^{*(i)})p(c_{k,k}^{*(i)})p(x_{k,k}^{*(i)} | x_{k,k-1}^{*(i)}, d_{k,k}^{*(i)})}{q(d_{k,k}^{*(i)} | x_{k,k-1}^{*(i)}, z_k)q(c_{k,k}^{*(i)} | x_{k,k-1}^{*(i)}, d_{k,k}^{*(i)})} \frac{q(d_{k,k}^{i-1} | x_{k,k-1}^{i-1}, z_k)q(c_{k,k}^{i-1} | x_{k,k-1}^{i-1}, d_{k,k}^{i-1})}{p(d_{k,k}^{i-1})p(c_{k,k}^{i-1})p(x_{k,k}^{i-1} | x_{k,k-1}^{i-1}, d_{k,k}^{i-1})} \frac{|\det(C^{*(i)})|p(\bar{\eta}_0^{i-1} | x_{k,k-1}^{i-1}, d_{k,k}^{i-1})p(z_k | x_{k,k}^{*(i)}, c_{k,k}^{*(i)})}{p(\bar{\eta}_0^{*(i)} | x_{k,k-1}^{*(i)}, d_{k,k}^{*(i)})|\det(C^{i-1})|p(z_k | x_{k,k}^{i-1}, c_{k,k}^{i-1})} \right)$;
- 8: Accept $x_{k,0:k}^i = x_{k,0:k}^{*(i)}$, $\eta_0^i = \eta_0^{*(i)}$, $d_{k,k}^i = d_{k,k}^{*(i)}$, $c_{k,k}^i = c_{k,k}^{*(i)}$, $C^i = C^{*(i)}$ and $D^i = D^{*(i)}$ with probability ρ_1 . Otherwise set $x_{k,0:k}^i = x_{k,0:k}^{i-1}$, $\eta_0^i = \eta_0^{i-1}$, $d_{k,k}^i = d_{k,k}^{i-1}$, $c_{k,k}^i = c_{k,k}^{i-1}$, $C^i = C^{i-1}$ and $D^i = D^{i-1}$;
- 9: Individual refinements of $x_{k,0:k}^i$ using Algorithm 5 given $d_{k,k}^i$ and $c_{k,k}^i$;
- 10: Calculate $\eta_0^i = (C^i)^{-1}(x_{k,k}^i - D^i)$;

simplicity. The results are, however valid for any non-zero N_b . Our results are derived for Algorithms 1, 2, 4 and 6. However, they can be easily extended to apply to Algorithm 8 as well, by considering convergence in the extended state space $(x_{0:k}, d_{1:k}, c_{1:k})$ which implies convergence of $x_{0:k}$.

We assume that $\pi_k(x_{0:k})$ is defined on a measurable space (E_k, \mathcal{F}_k) where $E_0 = E$, $\mathcal{F}_0 = \mathcal{F}$, and $E_k = E_{k-1} \times E$, $\mathcal{F}_k = \mathcal{F}_{k-1} \times \mathcal{F}$. We denote by $\mathcal{P}(E_k)$ the set of probability measures on (E_k, \mathcal{F}_k) . We also define $\mathcal{S}_k = \{x_{0:k} \in E_k : \pi_k(x_{0:k}) > 0\}$. For $k \geq 0$, π_k is known up to a normalizing constant $0 < Z_k < \infty$. We have

$$\pi_k(x_{0:k}) = \frac{p(x_0) \prod_{l=1}^k p(x_l | x_{l-1})p(z_l | x_l)}{p(z_{1:k})} = \frac{\gamma_k(x_{0:k})}{Z_k}, \quad (37)$$

where $\gamma_k : E_k \rightarrow \mathbb{R}^+$ is known point-wise and the normalizing constant $Z_k = \int_{E_k} \gamma_k(dx_{0:k}) = p(z_{1:k})$ is the unknown marginal likelihood of the observations. For the joint draw step in SMC MC, the proposal distribution at time $k = 0$ is $q_0(x_0)$, and for $k > 0$ it is $q_k(x_{0:k-1}, x_k)$, where $q_k : \mathbb{E}_{k-1} \times \mathbb{E} \rightarrow \mathbb{R}^+$ is a probability density in its last argument x_k conditional on its previous arguments $x_{0:k-1}$. For $k > 0$ and for any measure $\mu_{k-1} \in \mathcal{P}(E_{k-1})$, we define

$$(\mu_{k-1} \times q_k)(dx_{0:k}) = \mu_{k-1}(dx_{0:k-1})q_k(x_{0:k-1}, dx_k). \quad (38)$$

Based on the proposal distributions $q_0(x_0)$ and $q_k(x_{0:k-1}, x_k)$, we define importance weights:

$$w_0(x_0) = \frac{\gamma_0(x_0)}{q_0(x_0)}; \quad (39)$$

and for $k > 0$

$$w_k(x_{0:k}) = \frac{\gamma_k(x_{0:k})}{\gamma_{k-1}(x_{0:k-1})q_k(x_{0:k-1}, x_k)}. \quad (40)$$

Combining Equations (37), (38), (39) and (40), it is easy to derive that

$$Z_0 = \int_{E_0} w_0(x_0)q_0(dx_0), \quad (41)$$

and for $k > 0$

$$\frac{Z_k}{Z_{k-1}} = \int_{E_k} w_k(x_{0:k})(\pi_{k-1} \times q_k)(dx_{0:k}). \quad (42)$$

Asymptotically, $x_{0:k}^{*(i)}$ is distributed according to $(\pi_{k-1} \times q_k)(x_{0:k})$. Thus, the (ratio of) normalizing constants can easily be estimated as

$$\widehat{Z}_0^{(N_p)} = \frac{1}{N_p} \sum_{i=1}^{N_p} w_0(x_0^{*(i)}), \quad (43)$$

and for $k > 0$

$$\left(\frac{Z_k}{Z_{k-1}} \right)^{(N_p)} = \frac{1}{N_p} \sum_{i=1}^{N_p} w_k(x_{0:k}^{*(i)}). \quad (44)$$

We use $\widehat{\pi}_k^{(N_p)}(x_{0:k})$ to denote the empirical measure approximation of the target distribution $\pi_k(x_{0:k})$.

$$\widehat{\pi}_k^{(N_p)}(x_{0:k}) = \frac{1}{N_p} \sum_{i=1}^{N_p} \delta_{x_{0:k}^{*(i)}}(x_{0:k}). \quad (45)$$

For any measure μ and integrable test function $f : E \rightarrow \mathbb{R}$, we define $\mu(f) = \int_E f(x)\mu(dx)$. We denote that $\mathcal{L}^p(E_k, \mathcal{F}_k, \mu_k) = \{f_k : E_k \rightarrow \mathbb{R} \text{ such that } f_k \text{ is measurable with respect to } \mathcal{F}_k \text{ and } \mu_k(|f_k|^p) < \infty\}$ for $p \geq 1$. In other words, $\mathcal{L}^p(E_k, \mathcal{F}_k, \mu_k)$ is the set of real-valued, \mathcal{F}_k -measurable functions defined on E_k , whose absolute p 'th moment exists with respect to μ_k .

The following theorem requires the following relatively weak assumption to be satisfied:

Assumption 1. For any time index $k \geq 0$, there exists $B_k < \infty$ such that for any $x_{0:k} \in \mathcal{S}_k$, we have $w_k(x_{0:k}) \leq B_k$.

Our first result establishes almost sure convergence of the approximating distribution to the target distribution. See Appendix A for the proof of the theorem.

Theorem IV.1. Given Assumption 1, for any $k \geq 0$, $x_{0:l}^{(0)} \in \mathcal{S}_l$ for $0 \leq l \leq k$ and $f_k \in \mathcal{L}^1(E_k, \mathcal{F}_k, \pi_k)$,

$$\widehat{\pi}_k^{(N_p)}(f_k) \rightarrow \pi_k(f_k) \quad (46)$$

almost surely, as $N_p \rightarrow \infty$.

With Equations (43) and (44), a straightforward corollary of Theorem IV.1 follows. See Appendix B for the proof.

Corollary IV.1.1. Given Assumption 1, for any $k \geq 0$ and $x_{0:l}^{(0)} \in \mathcal{S}_l$ for $0 \leq l \leq k$,

$$\widehat{Z}_0^{(N_p)} \rightarrow Z_0, \quad (47)$$

and for $k > 0$,

$$\left(\frac{Z_k}{Z_{k-1}} \right)^{(N_p)} \rightarrow \frac{Z_k}{Z_{k-1}}, \quad (48)$$

almost surely, as $N_p \rightarrow \infty$.

V. SIMULATION AND RESULTS

In this section we describe the numerical simulation experiments that we have conducted to evaluate the performance of the proposed algorithms. The experiments explore idealized scenarios in order to focus on the sampling capabilities of the compared algorithms. More extensive experimentation is required to explore the impact of practical issues in sensor networks.

A. Large spatial sensor networks example

We first examine the proposed algorithms in simulations with setups of large spatial sensor networks. d sensors are evenly deployed on a two-dimensional grid, at coordinates $\{1, 2, \dots, \sqrt{d}\} \times \{1, 2, \dots, \sqrt{d}\}$. Each sensor collects measurements independently with respect to the other sensors, about the underlying states at the sensor's location. Such networks can be useful in environment monitoring, weather forecasts and surveillance.

The SmHMC algorithm leads to the smallest average mean squared error in these large spatial sensor network examples [33], hence we would like to evaluate the proposed algorithms in the same examples.

The full state at time step k is denoted by $x_k = [x_k^1, \dots, x_k^d]$, where $x_k^s \in \mathbb{R}$ is the state at the s -th sensor's position for $s \in \{1, \dots, d\}$. x_k evolves according to a multivariate Generalized Hyperbolic (GH) skewed- t distribution, which is a heavy-tailed distribution useful for modeling physical processes, extreme events and financial markets [40]:

$$p(x_k | x_{k-1}) = \frac{e^{(x_k - \alpha x_{k-1})^T \Sigma^{-1} \gamma}}{\sqrt{(\nu + Q(x_k))(\gamma^T \Sigma^{-1} \gamma)}^{-\frac{\nu+d}{2}} \left(1 + \frac{Q(x_k)}{\nu}\right)^{\frac{\nu+d}{2}}} \times K_{\frac{\nu+d}{2}} \left(\sqrt{(\nu + Q(x_k))(\gamma^T \Sigma^{-1} \gamma)} \right). \quad (49)$$

Here α is a scalar, the parameters γ and ν determine the shape of the distribution, $K_{\frac{\nu+d}{2}}$ is the modified Bessel function of the second kind of order $\frac{\nu+d}{2}$, and $Q(x_k) = (x_k - \alpha x_{k-1})^T \Sigma^{-1} (x_k - \alpha x_{k-1})$. The (i, j) -th entry of the dispersion matrix Σ is defined by:

$$\Sigma_{i,j} = \alpha_0 e^{-\frac{\|L^i - L^j\|_2^2}{\beta}} + \alpha_1 \delta_{i,j}. \quad (50)$$

We use $\|\cdot\|_2$ to denote the L2-norm. L^i is the physical location of the i -th sensor, and $\delta_{i,j}$ is the Kronecker symbol.

The measurements are Poisson-distributed count data:

$$p(z_k | x_k) = \prod_{s=1}^d \mathcal{P}(z_k^s; m_1 e^{m_2 x_k^s}). \quad (51)$$

$\mathcal{P}(\cdot; \Lambda)$ denotes the Poisson(Λ) distribution. m_1 and m_2 are scalars which control the mean of the Poisson distribution.

We set $\alpha = 0.9$, $\alpha_0 = 3$, $\alpha_1 = 0.01$, $\beta = 20$, $\nu = 7$, $m_1 = 1$ and $m_2 = \frac{1}{3}$. All elements of the vector γ are set to 0.3. d is set to 144 or 400 to represent two high-dimensional filtering examples. Each simulation example is executed for 100 times and each simulation lasts for 10 time steps. Execution time in this paper is produced with an Intel i7-4770K 3.50GHz CPU and 32GB RAM. Where not specified otherwise, the number of samples N_p is 200, and the burn-in period is 20.

Table I reports the average estimation errors, acceptance rates (if applicable) and execution time. We observe that by combining SmHMC with the EDH flow (SmHMC (EDH)) or the LEDH flow (SmHMC (LEDH)), the average MSE decreases compared with the vanilla SmHMC algorithm where the independent MH kernel based on prior as proposal is employed in the joint draw step. The decrease in the MSE is due to the increase of the acceptance ratio in the joint draw step where particle flow is employed. So, samples are more diversified after the joint draw step. The SmHMC (EDH) and SmHMC (LEDH) algorithms lead to similar average MSEs. The SmHMC (EDH) algorithm is hence preferred in this setting as it is computationally much more efficient than the SmHMC (LEDH) method. The SmHMC (LEDH) method adds negligible computational overhead compared to the SmHMC.

The EDH and the LEDH methods produce similar MSEs, again indicating that performing separate flow parameters for each particle does not offer additional gain in this setting. Although the MSEs from the EDH and the LEDH are the smallest among compared algorithms, these two algorithms are not statistically consistent. The PF-PF based on the EDH flow has a higher MSE than SmHMC (EDH) with the same number of particles as although the EDH flow moves particles to region where posterior densities are relatively high, the particle filter can still suffer from weight degeneracy in such high-dimensional spaces. An increased number of particles lead to improved performance for PF-PF (EDH), but this requires a much higher consumption of memory due to flow operations of a large number particles. The bootstrap particle filter (BPF) produces high average MSE even with 1 million particles. The EKF and the UKF frequently lead to lost tracks as the posterior distributions are strongly non-Gaussian.

TABLE I
AVERAGE MSE, ACCEPTANCE RATES (IF APPLICABLE) AND EXECUTION TIME PER STEP IN THE LARGE SPATIAL SENSOR NETWORK EXAMPLE WITH A SKEWED - T DYNAMIC MODEL AND COUNT MEASUREMENTS. THE PARENTHESIS AFTER THE AVERAGE MSE VALUES INDICATES THE NUMBER OF LOST TRACKS OUT OF 100 SIMULATION TRIALS WHERE LOST TRACKS ARE DEFINED AS THOSE WHOSE AVERAGE ESTIMATION ERRORS ARE GREATER THAN $\frac{\sqrt{d}}{2}$. THE AVERAGE MSE IS CALCULATED WITH THE SIMULATION TRIALS WHERE TRACKING IS NOT LOST.

d	Algorithm	No. of particles	Avg. MSE	Acceptance rate			Exec. time (s)
				ρ_1	ρ_2	ρ_3	
144	SmHMC (EDH)	200	0.75	0.04	0.01	0.71	11.5
	SmHMC (LEDH)	200	0.76	0.05	0.01	0.71	19
	SmHMC	200	0.82	0.003	0.01	0.73	11
	EDH	200	0.68	-	-	-	0.05
	EDH	10000	0.68	-	-	-	0.6
	LEDH	200	0.71	-	-	-	7
	PF-PF (EDH)	200	0.88	-	-	-	0.05
	PF-PF (EDH)	10^5	0.73	-	-	-	6.0
	EKF	N/A	2.5 (28)	-	-	-	0.002
	UKF	N/A	2.4 (34)	-	-	-	0.05
	BPF	10^6	1.4 (1)	-	-	-	6.8
	400	SmHMC (EDH)	200	0.70	0.02	0.02	0.61
SmHMC (LEDH)		200	0.71	0.02	0.02	0.60	205
SmHMC		200	0.73	0.002	0.02	0.63	88
EDH		200	0.60	-	-	-	0.5
EDH		10000	0.60	-	-	-	2.5
LEDH		200	0.62	-	-	-	88
PF-PF (EDH)		200	0.92	-	-	-	0.6
PF-PF (EDH)		10^5	0.75	-	-	-	21
EKF		N/A	3.4 (18)	-	-	-	0.03
UKF		N/A	3.8 (27)	-	-	-	1.2
BPF		10^6	3.3 (1)	-	-	-	23

B. Estimation of normalizing constants from a linear Gaussian example

In many Bayesian inference problems, it is very important to estimate the normalizing constant Z_k . For a general HMM, analytical evaluation of (41) and (42) is not possible, as π_{k-1} is not tractable. However, in a linear Gaussian filtering problem, the posterior distribution can be analytically computed from a Kalman filter, which allows exact estimation of Z_k . Here we consider a linear Gaussian setup to allow us to compare the estimated normalizing constants against the true values. The dynamic and measurement models are:

$$x_k = \alpha x_{k-1} + v_k, \quad (52)$$

$$z_k = x_k + w_k, \quad (53)$$

where $x_k \in \mathbb{R}^d$ and $z_k \in \mathbb{R}^d$ are the state and measurement vectors respectively. We set $\alpha = 0.9$ as in the previous section. The process noise $v_k \sim \mathcal{N}(\mathbf{0}, \Sigma)$ where Σ is given in (50). The measurement noise $w_k \sim \mathcal{N}(\mathbf{0}, \sigma_z^2 I)$. We set $\sigma_z = 0.5$. The true state starts at $x_0 = \mathbf{0}$. We set $d = 64$. The experiment is executed 100 times for $T = 10$ time steps.

The main objective of this experiment is to compare SMCMC algorithms with different particle filters for estimation of normalizing constants. We define the relative MSE in estimating $\log Z_k$ as follows:

$$MSE_{\log Z}^{(rel)} = \frac{\sum_{k=1}^T (\log Z_k - \log \widehat{Z}_k)^2}{\sum_{k=1}^T (\log Z_k)^2}.$$

For this linear Gaussian setup, the Kalman filter (KF), shows the least error in state estimation in Table II. It also can compute $\log Z_k$ analytically. The average acceptance rates of the SmHMC (LEDH) and SmHMC (EDH) are higher than the vanilla SmHMC, showing that the incorporation of particle flow in SmHMC provides many more initializations for mHMC based refinement and better mixing. Although the average error in the state estimation is almost the same for all SMC algorithms because of the effectiveness of mHMC, the poor performance of SmHMC in estimating $\log Z_k$ shows that the independent MH kernel based on prior as proposal, which is employed in joint draw of SmHMC, is inefficient in this high-dimensional example. We also note that SmHMC (LEDH) and SmHMC (EDH) perform similarly to the PFPF (LEDH) and PFPF (EDH) [24] for the same number of particles. However, estimation of $\log Z_k$ can be improved significantly by increasing the number of particles in PFPF (EDH), with negligible computational overhead. The BPF suffers from severe weight degeneracy and shows poor estimation performance, even if a large number of particles is employed.

TABLE II
AVERAGE MSE, $MSE_{\log Z}^{(rel)}$, ESS (IF APPLICABLE) AND EXECUTION TIME PER STEP IN THE LINEAR GAUSSIAN EXAMPLE.

Algorithm	No. of particles	Avg. MSE	Avg. $MSE_{\log Z}^{(rel)}$	Avg. ESS	Exec. time (s)
KF	N/A	0.07	0	-	0.002
SmHMC (LEDH)	200	0.08	0.0006	-	2.5
SmHMC (EDH)	200	0.08	0.0006	-	0.70
SmHMC	200	0.09	1.629	-	0.6
PFPF (LEDH)	200	0.09	0.0005	25.1	1.90
PFPF (EDH)	200	0.09	0.0006	21.7	0.015
PFPF (EDH)	10^4	0.08	0.0001	852	0.2
BPF	200	1.10	2.813	1.04	0.001
BPF	10^6	0.20	0.0265	1.62	2.5

C. Nonlinear model with GMM process and measurement noises

Here we consider a nonlinear dynamical model $g_k : \mathbb{R}^d \rightarrow \mathbb{R}^d$ and measurement function $h_k : \mathbb{R}^d \rightarrow \mathbb{R}^d$. The c -th element of the measurement vector is $h_k^c(x_k) = \frac{(x_k^c)^2}{20}$, $\forall 1 \leq c \leq d$. c -th element of the state vector is defined as follows:

$$g_k^c(x_{k-1}) = 0.5x_{k-1}^c + 8 \cos(1.2(k-1)) + \begin{cases} 2.5 \frac{x_{k-1}^{c+1}}{1+(x_{k-1}^c)^2} & , \text{ if } c = 1 \\ 2.5 \frac{x_{k-1}^{c+1}}{1+(x_{k-1}^{c-1})^2} & , \text{ if } 1 < c < d \\ 2.5 \frac{x_{k-1}^c}{1+(x_{k-1}^{c-1})^2} & , \text{ if } c = d \end{cases} \quad (54)$$

Process noise $v_k \sim \sum_{m=1}^3 \frac{1}{3} \mathcal{N}(\mu_m \mathbf{1}_{d \times 1}, \sigma_v^2 I_{d \times d})$, with $\mu_1 = -1$, $\mu_2 = 0$, $\mu_3 = 1$ and $\sigma_v = 0.5$, and measurement noise $w_k \sim \sum_{n=1}^3 \frac{1}{3} \mathcal{N}(\delta_n \mathbf{1}_{d \times 1}, \sigma_w^2 I_{d \times d})$, with $\delta_1 = -3$, $\delta_2 = 0$, $\delta_3 = 3$ and $\sigma_w = 0.1$. The true state starts at $x_0 = \mathbf{0}$. For all the filters, we use $p(x_0) = \mathcal{N}(\mathbf{0}_{d \times 1}, I_{d \times d})$. The experiment is executed 100 times for 50 time steps. We perform two different experiments with $d = 144$ and $d = 400$.

TABLE III
AVERAGE MSE, ACCEPTANCE RATES (IF APPLICABLE) AND EXECUTION TIME PER STEP IN THE NONLINEAR MODEL WITH GMM PROCESS AND MEASUREMENT NOISES, BASED ON 100 SIMULATION TRIALS.

d	Algorithm	No. of particles	Avg. MSE	Acceptance rate			Exec. time (s)
				ρ_1	ρ_2	ρ_3	
144	SmHMC-GMM (LEDH)	100	0.10	0.072	0.17	0.74	7.12
	SmHMC-GMM	100	0.12	0.005	0.17	0.76	3.3
	PFPF-GMM	200	0.10	-	-	-	7.4
	PF-GMM	50 per comp.	0.18	-	-	-	12.4
	GSPF	10^4 per comp.	4.53	-	-	-	3.7
	EKF-GMM	N/A	2.12	-	-	-	0.05
	UKF	N/A	1.30	-	-	-	0.15
	LEDH	500	9.05	-	-	-	13.9
	EDH	500	11.54	-	-	-	0.04
	PFPF (LEDH)	500	5.90	-	-	-	19
	PFPF (EDH)	10^5	3.01	-	-	-	4.60
	BPF	10^6	0.94	-	-	-	9
400	SmHMC-GMM (LEDH)	100	0.09	0.018	0.096	0.60	59.5
	SmHMC-GMM	100	0.11	0.005	0.085	0.64	13.3
	PFPF-GMM	200	0.11	-	-	-	80.2
	PF-GMM	50 per comp.	0.11	-	-	-	142.7
	GSPF	10^4 per comp.	5.17	-	-	-	9.4
	EKF-GMM	N/A	1.61	-	-	-	0.3
	UKF	N/A	5.18	-	-	-	1.37
	LEDH	500	23.42	-	-	-	152.6
	EDH	500	30.45	-	-	-	0.42
	PFPF (LEDH)	500	16.38	-	-	-	194
	PFPF (EDH)	10^5	12.27	-	-	-	16.8
	BPF	10^6	1.31	-	-	-	26.2

Table III shows that while the proposed SmHMC-GMM (LEDH) achieves the same smallest average MSE as the PFPF-GMM [38] algorithm among all evaluated methods in the 144 dimensional scenario, the SmHMC-GMM (LEDH) leads to the smallest average MSE in the 400 dimensional scenario. The SmHMC-GMM is an SmHMC variant such that after sampling of (d_k, c_k) using the same distributions as in SmHMC-GMM (LEDH) in the joint draw, x_k is proposed using the particular component of the dynamic model specified by d_k . The comparison of acceptance rates in the joint draw and MSE for these two algorithms shows that the use of particle flow in the SmHMC-GMM (LEDH) method allows it to explore the state space more efficiently than the SmHMC-GMM algorithm.

The PF-GMM [41], which uses a separate LEDH filter to track each component of the posterior, performs reasonably well, whereas the particle flow algorithms LEDH, EDH and the particle flow particle filters perform poorly as they are better suited for uni-modal posterior distributions. The Gaussian sum particle filter (GSPF) [42], which approximates each component of the predictive and posterior densities by a Gaussian distribution by performing importance sampling exhibits poor representation capability in higher dimensions. The extended Kalman filter for GMM noises (EKF-GMM) and

UKF lead to large estimation errors. The BPF also has high MSE even with 10^6 particles, due to the weight degeneracy in the high-dimensional state space.

VI. CONCLUSION

In this paper, we proposed a series of composite MH kernels for SMCMC methods. These kernels are constructed based on invertible particle flow to achieve efficient exploration of high-dimensional state spaces. The EDH-based SMCMC method provides minimal computational overhead but a significant increase of the acceptance rate in the joint draw compared to the state-of-the-art SMCMC algorithm, the SmHMC method. For multi-modal distributions, a Gaussian mixture model-based particle flow is incorporated to migrate samples into high posterior density regions. Theoretical convergence results are also derived for the SMCMC methods.

We evaluated the proposed algorithms in three simulation examples. In the large spatial sensor network setup with high-dimensional non-Gaussian distributions, the EDH and the LEDH methods provide the smallest MSEs, but there are no convergence results for these flow-based algorithms. The SmHMC methods based on the EDH or the LEDH flow have been shown in the paper to converge to the target distribution, and in the 400-dimensional filtering example, they provide the smallest MSEs among all particle filters and SmHMC algorithms for which convergence results have been established. In the linear Gaussian example, both the SmHMC (EDH) and the SmHMC (LEDH) methods provide smaller estimation errors of the normalisation constants compared to SmHMC. In the third example with high-dimensional nonlinear HMM models and GMM process and measurement noise, the proposed SmHMC-GMM (LEDH) algorithm provides the smallest estimation errors in both the 144-dimensional and 400-dimensional experiment settings.

An important future research direction is a more extensive experimental evaluation of flow-based SMCMC algorithms. These experiments should investigate the impact of the initial state values, the process noise variance, the measurement noise variance, coupling in the dynamic models, partial observations, the data rate and measurement uncertainty. Such experiments can shed light on the robustness of the invertible particle flow-based approach in practical applications and motivate the development of new algorithms that address any exposed deficiencies. One example of the real-world challenges in sensor networks is data incest due to the inadvertent re-use of the same measurements [43], which can be mitigated to some extent by a data incest management strategy that takes into account the network topology [44] or information fusion techniques with copula processes [45].

Other problems common in practical sensor networks are missed detections, false alarms, and finite measurement resolution. Addressing such practical problems is important and can lead to interesting research directions, e.g., designing an appropriate combination of sequential MCMC, particle flow and random finite sets.

Beyond experimentation, there are important methodological and theoretical issues to explore in future work. In terms

of particle flow, the algorithms in this paper use deterministic flows in order to obtain an invertible mapping. It is more challenging to incorporate stochastic particle flow, but the stochastic flow algorithms have been demonstrated to achieve considerably better performance [18], so integration is desirable. The stiffness of the differential equations is an issue in both particle flow and Hamiltonian Monte Carlo and can lead to numerical instability. For this reason, and also to guarantee the invertible mapping property for the flows, we use a very small step size in the particle flow procedure. This leads to a greater computational overhead. Alternative strategies for addressing stiffness have been proposed in [17], [18], and it would be interesting to explore their incorporation in the flow-based SMCMC framework. This paper derives the asymptotic convergence results of the proposed algorithms. Finite sample analysis of filter errors is an important direction to explore; [36] provides a valuable finite sample bound for SMCMC errors. In a similar manner to [46], it may be possible to identify a relationship between the magnitude of the error and the stiffness of the flow.

APPENDIX A PROOF OF THEOREM IV.1

We start with several notations and propositions. For $k > 0$, the proposal distribution q_k^{opt} that minimizes the variance of importance weights is the conditional density of x_k given $x_{0:k-1}$ under π_k [35].

$$\begin{aligned} q_k^{opt}(x_{0:k-1}, x_k) &= \bar{\pi}_k(x_{0:k-1}, x_k) := \frac{\pi_k(x_{0:k})}{\pi_k(x_{0:k-1})}, \\ &= p(x_k | x_{0:k-1}, z_k), \end{aligned} \quad (55)$$

where $\pi_k(x_{0:k-1}) = \int_E \pi_k(x_{0:k}) dx_k$.

With this ‘‘optimal’’ density, the optimal importance weight w_k^{opt} does not depend on x_k .

$$\begin{aligned} w_k^{opt}(x_{0:k}) &\propto \pi_{k/k-1}(x_{0:k-1}), \\ &:= \frac{\pi_k(x_{0:k-1})}{\pi_{k-1}(x_{0:k-1})} = p(z_k | x_{k-1}). \end{aligned} \quad (56)$$

In the SMCMC algorithm, at iteration i of any given time step k , there is a joint draw of $x_{0:k}^i$ which is then followed by individual refinements of $x_{0:k}^{(i)}$ using the *Metropolis within Gibbs* technique, if $k > 0$. There is no refinement step at time $k = 0$. Using Equations (4), (5), (39) and (40), we calculate the acceptance probability of the joint draw as follows:

$$\begin{aligned} \alpha_0(x_0^{i-1}, x_0^{*(i)}) &= \min \left(1, \frac{\pi_0(x_0^{*(i)}) q_0(x_0^{i-1})}{q_0(x_0^{*(i)}) \pi_0(x_0^{i-1})} \right), \\ &= \min \left(1, \frac{w_0(x_0^{*(i)})}{w_0(x_0^{i-1})} \right), \end{aligned} \quad (57)$$

and for $k > 0$,

$$\begin{aligned}
& \alpha_k(x_{0:k}^{i-1}, x_{0:k}^{*(i)}) \\
&= \min \left(1, \frac{\check{\pi}_k(x_{0:k}^{*(i)}) \widehat{\pi}_{k-1}^{(N_p)}(x_{0:k-1}^{i-1}) q_k(x_{0:k-1}^{i-1}, x_k^{i-1})}{\widehat{\pi}_{k-1}^{(N_p)}(x_{0:k-1}^{*(i)}) q_k(x_{0:k-1}^{*(i)}, x_k^{*(i)}) \check{\pi}_k(x_{0:k}^{i-1})} \right), \\
&= \min \left(1, \frac{\pi_k(x_{0:k}^{*(i)}) \pi_{k-1}(x_{0:k-1}^{i-1}) q_k(x_{0:k-1}^{i-1}, x_k^{i-1})}{\pi_{k-1}(x_{0:k-1}^{*(i)}) q_k(x_{0:k-1}^{*(i)}, x_k^{*(i)}) \pi_k(x_{0:k}^{i-1})} \right), \\
&= \min \left(1, \frac{w_k(x_{0:k}^{*(i)})}{w_k(x_{0:k}^{i-1})} \right). \tag{58}
\end{aligned}$$

We define the independent MH kernel to initialize the algorithm, $K_0^{draw} : E_0 \times \mathcal{F}_0 \rightarrow [0, 1]$:

$$\begin{aligned}
K_0^{draw}(x_0, dx'_0) &= \alpha_0(x_0, x'_0) q_0(dx'_0) \\
&+ \left(1 - \int_{E_0} \alpha_0(x_0, y_0) q_0(dy_0) \right) \delta_{x_0}(dx'_0). \tag{59}
\end{aligned}$$

For $k > 0$, we use $\widehat{\pi}_{k-1}^{(N_p)} \in \mathcal{P}_{k-1}(E_{k-1})$ to construct the joint proposal $(\widehat{\pi}_{k-1}^{(N_p)} \times q_k)$ for the joint draw, which is associated with the Markov kernel $K_k^{draw} : E_k \times \mathcal{F}_k \rightarrow [0, 1]$, defined by

$$\begin{aligned}
K_k^{draw}(x_{0:k}, dx'_{0:k}) &= \alpha_k(x_{0:k}, x'_{0:k}) (\widehat{\pi}_{k-1}^{(N_p)} \times q_k)(dx'_{0:k}) \\
&+ \left(1 - \int_{E_k} \alpha_k(x_{0:k}, y_{0:k}) (\widehat{\pi}_{k-1}^{(N_p)} \times q_k)(dy_{0:k}) \right) \delta_{x_{0:k}}(dx'_{0:k}). \tag{60}
\end{aligned}$$

Lemma A.1. *Given Assumption 1, $K_0^{draw}(x_0, dx'_0)$ is an independent Metropolis kernel, uniformly ergodic of invariant distribution $\pi_0(dx_1)$.*

Proof. From Equation (57), we see that K_0^{draw} is an independent Metropolis kernel with target distribution π_0 and proposal q_0 . If Assumption 1 is satisfied, uniform ergodicity follows from Corollary 4 in [47]. \square

Proposition 1. *Given Assumption 1, for any $k > 0$, $K_k^{draw}(x_{0:k}, dx'_{0:k})$ is uniformly ergodic of invariant distribution*

$$\check{\pi}_k^{(N_p)}(dx_{0:k}) = \frac{\pi_{k/k-1}(x_{0:k-1}) \cdot (\widehat{\pi}_{k-1}^{(N_p)} \times \bar{\pi}_k)(dx_{0:k})}{\widehat{\pi}_{k-1}^{(N_p)}(\pi_{k/k-1})}, \tag{61}$$

where $\bar{\pi}_k(x_{0:k-1}, dx_k)$ and $\pi_{k/k-1}(x_{0:k-1})$ are defined by Equations (55) and (56), respectively.

Proof. From Equation (58), we see that K_k^{draw} is an independent Metropolis kernel with target distribution $\check{\pi}_k^{(N_p)}$ and

proposal $\widehat{\pi}_{k-1}^{(N_p)} \times q_k$. From Equations (4), (5), (55) and (56) we have

$$\begin{aligned}
& \check{\pi}_k^{(N_p)}(x_{0:k}) \\
&= \frac{\pi_{k/k-1}(x_{0:k-1}) \bar{\pi}_k(x_{0:k-1}, x_k) \widehat{\pi}_{k-1}^{(N_p)}(x_{0:k-1})}{\int_{E_k} \pi_{k/k-1}(x_{0:k-1}) \bar{\pi}_k(x_{0:k-1}, x_k) \widehat{\pi}_{k-1}^{(N_p)}(x_{0:k-1}) dx_{0:k}}, \\
&= \frac{\pi_{k/k-1}(x_{0:k-1}) \cdot (\widehat{\pi}_{k-1}^{(N_p)} \times \bar{\pi}_k)(x_{0:k})}{\int_{E_{k-1}} \pi_{k/k-1}(x_{0:k-1}) \widehat{\pi}_{k-1}^{(N_p)}(x_{0:k-1}) dx_{0:k-1}}, \\
&= \frac{\pi_{k/k-1}(x_{0:k-1}) \cdot (\widehat{\pi}_{k-1}^{(N_p)} \times \bar{\pi}_k)(x_{0:k})}{\widehat{\pi}_{k-1}^{(N_p)}(\pi_{k/k-1})}. \tag{62}
\end{aligned}$$

\square

We denote the cumulative MCMC kernel of all the refinement steps by $K_k^{refine} : E_k \times \mathcal{F}_k \rightarrow [0, 1]$ for $k > 0$. We note that K_k^{refine} also has the same invariant distribution $\check{\pi}_k^{(N_p)}$, like K_k^{draw} . We define the overall MCMC kernel for SMC, $K_k : E_k \times \mathcal{F}_k \rightarrow [0, 1]$ for $k \geq 0$ as follows,

$$K_0(x_0, dx'_0) := K_0^{draw}(x_0, dx'_0), \tag{63}$$

and for $k > 0$,

$$\begin{aligned}
K_k(x_{0:k}, dx'_{0:k}) &:= K_k^{refine} K_k^{draw}(x_{0:k}, dx'_{0:k}), \\
&= \int_{E_k} K_k^{refine}(y_{0:k}, dx'_{0:k}) K_k^{draw}(x_{0:k}, dy_{0:k}). \tag{64}
\end{aligned}$$

Proposition 2. *For any $k \geq 0$, $K_k(x_{0:k}, dx'_{0:k})$ is uniformly ergodic of invariant distribution $\check{\pi}_k^{(N_p)}(dx_{0:k})$.*

Proof. For $k = 0$, the result is trivially true from the definition of K_0 in Equation (63) and Lemma A.1. For $k > 0$, the assertion follows from application of Corollary 4 and Proposition 4 in [47] to the definition of K_k in Equation (64). \square

Proposition 3. *Suppose $\pi \in \mathcal{P}(E)$ and $K : E \times \mathcal{F} \rightarrow [0, 1]$ is an ergodic MCMC kernel of invariant distribution $\pi(dx)$. For any $f : E \rightarrow \mathbb{R}$, if $f \in \mathcal{L}^1(E, \mathcal{F}, \pi)$, $\widehat{\pi}^{(N_p)}(f)$ converges to $\pi(f)$ almost surely, irrespective of the starting point of the Markov chain $x^{(0)}$.*

Proof. See Theorem 3 in [47]. \square

A. Proof of Theorem IV.1

Proof. We prove the theorem using induction over k . For $k = 0$, the theorem is trivially true which can be seen by applying Proposition 3 with Lemma A.1. Let us assume that the theorem is true for $k-1$. We consider the following decomposition and examine each term individually.

$$\begin{aligned}
\widehat{\pi}_k^{(N_p)}(f_k) - \pi_k(f_k) &= [\widehat{\pi}_k^{(N_p)}(f_k) - \check{\pi}_k^{(N_p)}(f_k)] \\
&+ [\check{\pi}_k^{(N_p)}(f_k) - \pi_k(f_k)]. \tag{65}
\end{aligned}$$

From Equation (61), we have

$$\lim_{N_p \rightarrow \infty} \check{\pi}_k^{(N_p)}(f_k) = \frac{\lim_{N_p \rightarrow \infty} \widehat{\pi}_{k-1}^{(N_p)}(\pi_{k/k-1} \bar{f}_k)}{\lim_{N_p \rightarrow \infty} \widehat{\pi}_{k-1}^{(N_p)}(\pi_{k/k-1})}, \tag{66}$$

where,

$$\bar{f}_k(x_{0:k-1}) = \int_E f_k(x_{0:k-1}, x_k) \bar{\pi}_k(x_{0:k-1}, dx_k). \quad (67)$$

We note that, from Equation (56),

$$\begin{aligned} \pi_{k-1}(\pi_{k/k-1}) &= \int_{E_{k-1}} \pi_k(dx_{0:k-1}), \\ &= \int_{E_k} \pi_k(dx_{0:k}) = 1, \end{aligned} \quad (68)$$

and from Equation (67),

$$\begin{aligned} \pi_{k-1}(\pi_{k/k-1} \bar{f}_k) &= \int_{E_{k-1}} \bar{f}_k(x_{0:k-1}) \pi_k(dx_{0:k-1}), \\ &= \int_{E_k} f_k(x_{0:k}) \pi_k(dx_{0:k}), \\ &= \pi_k(f_k) \leq \pi_k(|f_k|) < \infty, \end{aligned} \quad (69)$$

because $f_k \in \mathcal{L}^1(E_k, \mathcal{F}_k, \pi_k)$. As Theorem IV.1 holds for $k-1$, we have from Equations (68) and (69)

$$\hat{\pi}_{k-1}^{(N_p)}(\pi_{k/k-1}) \longrightarrow 1, \quad (70)$$

and

$$\hat{\pi}_{k-1}^{(N_p)}(\pi_{k/k-1} \bar{f}_k) \longrightarrow \pi_k(f_k), \quad (71)$$

almost surely, as $N_p \rightarrow \infty$ for any $x_{0:l}^{(0)} \in \mathcal{S}_l$ for $0 \leq l \leq k-1$. Applying Equation (66), this implies that

$$\lim_{N_p \rightarrow \infty} \hat{\pi}_k^{(N_p)}(f_k) - \pi_k(f_k) = 0, \quad (72)$$

almost surely.

In the SMC algorithm, at time step k , the MCMC kernel used to sample $\{x_{0:k}^i\}_{i=1}^{N_p}$ is K_k , which, from Proposition 2, is uniformly ergodic of invariant distribution $\check{\pi}_k^{(N_p)}$. The applicability of Proposition 3 depends on the integrability of f_k w.r.t. $\lim_{N_p \rightarrow \infty} \check{\pi}_k^{(N_p)}$. From (72), if $f_k \in \mathcal{L}^1(E_k, \mathcal{F}_k, \pi_k)$, we also have $f_k \in \mathcal{L}^1(E_k, \mathcal{F}_k, \lim_{N_p \rightarrow \infty} \check{\pi}_k^{(N_p)})$ with probability 1, which allows us to use Proposition 3 to obtain

$$\hat{\pi}_k^{(N_p)}(f_k) - \lim_{N_p \rightarrow \infty} \check{\pi}_k^{(N_p)}(f_k) \longrightarrow 0, \quad (73)$$

almost surely, as $N_p \rightarrow \infty$, for any $x_{0:k}^{(0)} \in \mathcal{S}_k$. We use the equivalence in (72) and the almost sure convergence in (73) in Equation (65) to complete the proof of the theorem. \square

APPENDIX B

PROOF OF COROLLARY IV.1.1

Proof. From Equation (41), we have $Z_0 = q_0(w_0)$, where $w_0 \in \mathcal{L}^1(E_0, \mathcal{F}_0, q_0)$, because of Assumption 1. A straightforward application of *Kolmogorov's Strong Law of Large Numbers* (SLLN) proves the Corollary for $k=0$.

For $k > 0$, from Equation (42), we have

$$\frac{Z_k}{Z_{k-1}} = (\pi_{k-1} \times q_k)(w_k) \leq B_k,$$

because of Assumption 1. As $\{x_{0:k}^{*(i)}\}_{i=1}^{N_p}$ are i.i.d samples from $\hat{\pi}_{k-1}^{(N_p)} \times q_k$, we have, from (44)

$$\begin{aligned} \left(\frac{Z_k}{Z_{k-1}} \right)^{(N_p)} &\longrightarrow \left(\lim_{N_p \rightarrow \infty} \hat{\pi}_{k-1}^{(N_p)} \times q_k \right)(w_k) \\ &= (\pi_{k-1} \times q_k)(w_k) = \frac{Z_k}{Z_{k-1}} \end{aligned}$$

almost surely, as $N_p \rightarrow \infty$ for any $x_{0:l}^{(0)} \in \mathcal{S}_l$ for $0 \leq l \leq k$. The first step follows from Kolmogorov's SLLN and the second step follows from Theorem IV.1. \square

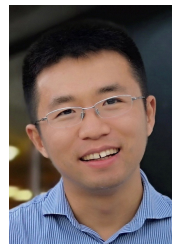
ACKNOWLEDGMENT

We acknowledge the support of the Natural Sciences and Engineering Research Council of Canada (NSERC) [2017-260250].

REFERENCES

- [1] R. Martinez-Cantin, N. de Freitas, E. Brochu, J. Castellanos, and A. Doucet, "A Bayesian exploration-exploitation approach for optimal online sensing and planning with a visually guided mobile robot," *Autonomous Robots*, vol. 27, no. 2, pp. 93–103, Aug 2009.
- [2] D. Creal and R. Tsay, "High dimensional dynamic stochastic copula models," *J. Econometrics*, vol. 189, no. 2, pp. 335–345, 2015.
- [3] S. Nannuru, Y. Li, Y. Zeng, M. Coates, and B. Yang, "Radio-frequency tomography for passive indoor multitarget tracking," *IEEE Trans. Mob. Comput.*, vol. 12, no. 12, pp. 2322–2333, Dec. 2013.
- [4] P. J. van Leeuwen, "Nonlinear data assimilation for high-dimensional systems," in *Nonlinear Data Assimilation*, P. J. van Leeuwen, C. Yuan, and S. Reich, Eds. Switzerland: Springer, 2015, ch. 1, pp. 1–73.
- [5] N. Gordon, D. Salmond, and A. Smith, "Novel approach to nonlinear/non-Gaussian Bayesian state estimation," in *IEE Proc. F Radar and Signal Process.*, vol. 140, no. 2, Apr. 1993, pp. 107–113.
- [6] A. Doucet and A. M. Johansen, "A tutorial on particle filtering and smoothing: Fifteen years later," in *The Oxford Handbook of Nonlinear Filtering*. Oxford, UK: Oxford University Press, 2009, ch. 24, pp. 656–704.
- [7] T. Bengtsson, P. Bickel, and B. Li, "Curse-of-dimensionality revisited: Collapse of the particle filter in very large scale systems," in *Probability and Statistics: Essays in Honor of David A. Freedman*, D. Nolan and T. Speed, Eds. Beachwood, OH: Institute of Mathematical Statistics, 2008, vol. 2, pp. 316–334.
- [8] C. Snyder, T. Bengtsson, P. Bickel, and J. Anderson, "Obstacles to high-dimensional particle filtering," *Mon. Weather Rev.*, vol. 136, no. 12, pp. 4629–4640, 2008.
- [9] A. Beskos, D. Crisan, and A. Jasra, "On the stability of sequential Monte Carlo methods in high dimensions," *Ann. Appl. Probab.*, vol. 24, no. 4, pp. 1396–1445, 2014.
- [10] A. Doucet, S. Godsill, and C. Andrieu, "On sequential Monte Carlo sampling methods for Bayesian filtering," *Stat. Comput.*, vol. 10, no. 3, pp. 197–208, 2000.
- [11] P. M. Djurić, T. Lu, and M. F. Bugallo, "Multiple particle filtering," in *Proc. Intl. Conf. Acoust., Speech and Signal Proc. (ICASSP)*, vol. 3, Apr. 2007, pp. 1181–1184.
- [12] P. Rebeschini and R. van Handel, "Can local particle filters beat the curse of dimensionality?" *Ann. Appl. Probab.*, vol. 25, no. 5, pp. 2809–2866, 10 2015.
- [13] A. Beskos, D. Crisan, A. Jasra, K. Kamatani, and Y. Zhou, "A stable particle filter for a class of high-dimensional state-space models," *Adv. Appl. Probab.*, vol. 49, no. 1, p. 2448, 2017.
- [14] M. Ades and P. J. van Leeuwen, "The equivalent-weights particle filter in a high-dimensional system," *Q. J. Royal Met. Soc.*, vol. 141, no. 1, pp. 484–503, 2015.
- [15] F. Daum and J. Huang, "Nonlinear filters with log-homotopy," in *Proc. SPIE Signal and Data Process. Small Targets*, San Diego, CA, Sep. 2007, p. 669918.
- [16] T. Ding and M. J. Coates, "Implementation of the Daum-Huang exact-flow particle filter," in *Proc. IEEE Statistical Signal Process. Workshop (SSP)*, Ann Arbor, MI, Aug. 2012, pp. 257–260.

- [17] F. Daum and J. Huang, "Seven dubious methods to mitigate stiffness in particle flow with non-zero diffusion for nonlinear filters, Bayesian decisions, and transport," in *Proc. SPIE Conf. Signal Proc., Sensor Fusion, Target Recog.*, Baltimore, MD, May 2014, p. 90920C.
- [18] F. Daum, J. Huang, and A. Noushin, "Generalized Gromov method for stochastic particle flow filters," in *Proc. SPIE Conf. Signal Proc., Sensor Fusion, Target Recog.*, Anaheim, CA, USA, May 2017, p. 102000I.
- [19] —, "Exact particle flow for nonlinear filters," in *Proc. SPIE Conf. Signal Proc., Sensor Fusion, Target Recog.*, Orlando, FL, Apr. 2010, p. 769704.
- [20] M. A. Khan and M. Ulmke, "Improvements in the implementation of log-homotopy based particle flow filters," in *Proc. Intl. Conf. Information Fusion*, July 2015, pp. 74–81.
- [21] S. Reich, "A guided sequential Monte Carlo method for the assimilation of data into stochastic dynamical systems," in *Recent Trends in Dynamical Systems*. Springer Basel, 2013, vol. 35, pp. 205–220.
- [22] J. Heng, A. Doucet, and Y. Pokern, "Gibbs flow for approximate transport with applications to Bayesian computation," *arXiv:1509.08787*, 2015.
- [23] P. Bunch and S. Godsill, "Approximations of the optimal importance density using Gaussian particle flow importance sampling," *J. Amer. Statist. Assoc.*, vol. 111, no. 514, pp. 748–762, 2016.
- [24] Y. Li and M. Coates, "Particle filtering with invertible particle flow," *IEEE Trans. Signal Process.*, vol. 65, no. 15, pp. 4102–4116, Aug. 2017.
- [25] C. Andrieu, N. de Freitas, A. Doucet, and M. I. Jordan, "An introduction to MCMC for machine learning," *Machine Learning*, vol. 50, no. 1, pp. 5–43, 2003.
- [26] S. Duane, A. D. Kennedy, B. J. Pendleton, and D. Roweth, "Hybrid Monte Carlo," *Phys. Lett. B*, vol. 195, no. 2, pp. 216 – 222, 1987.
- [27] R. M. Neal, "MCMC using Hamiltonian dynamics," in *Handbook of Markov Chain Monte Carlo*, S. Brooks, A. Gelman, G. L. Jones, and X. Meng, Eds. Boca Raton, USA: Chapman and Hall/CRC, 2011, ch. 5, pp. 113–162.
- [28] M. Girolami and B. Calderhead, "Riemann manifold Langevin and Hamiltonian Monte Carlo methods," *J. R. Stat. Soc. B*, vol. 73, no. 2, pp. 123–214, 2011.
- [29] M. Welling and Y. W. Teh, "Bayesian learning via stochastic gradient Langevin dynamics," in *Proc. Int. Conf. Machine Learning (ICML)*, Bellevue, USA, June 2011, pp. 681–688.
- [30] W. R. Gilks and C. Berzuini, "Following a moving target—Monte Carlo inference for dynamic Bayesian models," *J. R. Stat. Soc. B*, vol. 63, no. 1, pp. 127–146, 2001.
- [31] Z. Khan, T. Balch, and F. Dellaert, "MCMC-based particle filtering for tracking a variable number of interacting targets," *IEEE Trans. Pattern Anal. Mach. Intell.*, vol. 27, no. 11, pp. 1805–1819, Nov 2005.
- [32] F. Septier, S. K. Pang, A. Carmi, and S. Godsill, "On MCMC-based particle methods for Bayesian filtering: Application to multitarget tracking," in *Proc. Computational Advances in Multi-Sensor Adaptive Process. (CAMSAP)*, Aruba, The Netherlands, Dec. 2009, pp. 360–363.
- [33] F. Septier and G. W. Peters, "Langevin and Hamiltonian based sequential MCMC for efficient Bayesian filtering in high-dimensional spaces," *IEEE J. Sel. Topics Signal Process.*, vol. 10, no. 2, pp. 312–327, Mar. 2016.
- [34] Y. Li and M. Coates, "Sequential MCMC with invertible particle flow," in *Proc. Intl. Conf. Acoust., Speech and Signal Proc. (ICASSP)*, New Orleans, USA, Mar. 2017.
- [35] A. Brockwell, P. D. Moral, and A. Doucet, "Sequentially interacting Markov chain Monte Carlo methods," *Ann. Stat.*, vol. 38, no. 6, pp. 3387–3411, 2010.
- [36] A. Finke, A. Doucet, and A. M. Johansen, "Limit theorems for sequential MCMC methods," *arXiv e-prints, arXiv:1807.01057*, July 2018.
- [37] S. Choi, P. Willett, F. Daum, and J. Huang, "Discussion and application of the homotopy filter," in *Proc. SPIE Conf. Signal Proc., Sensor Fusion, Target Recog.*, Orlando, FL, May 2011, p. 805021.
- [38] S. Pal and M. Coates, "Particle flow particle filter for Gaussian mixture noise models," in *Proc. Intl. Conf. Acoust., Speech and Signal Proc. (ICASSP)*, Calgary, Canada, Apr. 2018.
- [39] M. Pitt and N. Shephard, "Filtering via simulation: Auxiliary particle filters," *J. Am. Statist. Assoc.*, vol. 94, no. 446, pp. 590–599, Jun. 1999.
- [40] D. Zhu and J. W. Galbraith, "A generalized asymmetric Student-t distribution with application to financial econometrics," *J. Econom.*, vol. 157, no. 2, pp. 297–305, 2010.
- [41] S. Pal and M. Coates, "Gaussian sum particle flow filter," in *Proc. Computational Advances in Multi-Sensor Adaptive Process.*, Curacao, The Netherlands, Dec. 2017.
- [42] J. H. Kotecha and P. M. Djuric, "Gaussian sum particle filtering," *IEEE Trans. Signal Process.*, vol. 51, no. 10, pp. 2602–2612, Oct 2003.
- [43] C. Fantacci, B. Vo, B. Vo, G. Battistelli, and L. Chisci, "Robust fusion for multisensor multiobject tracking," *IEEE Signal Proc. Lett.*, vol. 25, no. 5, pp. 640–644, May 2018.
- [44] T. Brehard and V. Krishnamurthy, "Optimal data incest removal in bayesian decentralized estimation over a sensor network," in *Proc. Intl. Conf. Acoust., Speech and Signal Proc. (ICASSP)*, vol. 3, Honolulu, Hawaii, USA, April 2007, pp. III–173–III–176.
- [45] J. Liu, I. Nevat, P. Zhang, and G. W. Peters, "Multimodal data fusion in sensor networks via copula processes," in *proc. IEEE Wireless Commun. Networking Conf. (WCNC)*, San Francisco, CA, USA, March 2017, pp. 1–6.
- [46] X. Cheng, N. S. Chatterji, P. L. Bartlett, and M. I. Jordan, "Underdamped Langevin MCMC: A non-asymptotic analysis," *arXiv:1707.03663*, Jul. 2017.
- [47] L. Tierney, "Markov chains for exploring posterior distributions," *Ann. Stat.*, vol. 22, no. 4, pp. 1701–1728, Dec 1994.



Yunpeng Li (S16) received the B.A. and M.S. Eng. degrees from the Beijing University of Posts and Telecommunications, Beijing, China, in 2009 and 2012, respectively, and the Ph.D. degree in the Department of Electrical and Computer Engineering at McGill University in Montreal, Quebec, Canada in 2017. From 2017 to 2018, he was Postdoctoral Research Assistant in Machine Learning at the Machine Learning Research Group, University of Oxford, Oxford, U.K. He was Junior Research Fellow at the Wolfson College, University of Oxford in 2018.

Since August 2018, he has been Lecturer in Artificial Intelligence in the Department of Computer Science at the University of Surrey, Guildford, U.K. His research interests include Bayesian inference, Monte Carlo methods, and statistical machine learning.



Soumyasundar Pal received the B.E. degree from the Jadavpur University, Kolkata, India in 2012 and the M.E. degree from the Indian Institute of Science, Bangalore, India, in 2014. Since 2016, he has been a Ph.D. student in the Department of Electrical and Computer Engineering at McGill University in Montreal, Quebec, Canada. His research interests include Bayesian inference, Monte Carlo methods, and machine learning on graphs.



Mark J. Coates (M'00-SM04) received the B.E. degree in computer systems engineering from the University of Adelaide, Adelaide, Australia, in 1995, and the Ph.D. degree from the University of Cambridge, Cambridge, U.K., in 1999. He joined McGill University, Montreal, Canada, in 2002, where he is currently a Professor in the Department of Electrical and Computer Engineering. He was a research associate and a Lecturer at Rice University, TX, USA, from 1999 to 2001. From 2012 to 2013, he worked as a Senior Scientist at Winton Capital

Management, Oxford, U.K. He currently serves as Associate Editor for IEEE TRANSACTIONS ON SIGNAL AND INFORMATION PROCESSING OVER NETWORKS. His research interests include statistical signal processing, machine learning, communication and sensor networks, and Bayesian and Monte Carlo inference.